ヒトES細胞由来分化細胞株から直接，あるいはヒトES細胞由来中間細胞株を経て，最終製品の構成要素となる細胞を作製する方法（分化誘導方法，目的とする細胞の分離・培養の方法，培養の各段階での培地，培養条件，培養期間及び収率等）を明確にし，その妥当性を明らかにすること。

(4) 細胞のバンク化

ヒトES細胞加工医薬品等の製造のいずれかの過程で，細胞をバンク化する場合には，その理由，セル・バンクの作製方法及びセル・バンクの特性解析（細胞純度，形態学的評価，表現型特異的マーカー，核型，細胞増殖特性，分化能など），保存・維持・管理方法・更新方法その他の各作業工程や試験に関する手順等について詳細を明らかにし，妥当性を示すこと。平成12年7月14日付け医薬審第873号厚生省医薬安全局審査管理課長通知「生物薬品（バイオテクノロジー応用医薬品／生物起源由来医薬品）製造用細胞基剤の由来，調製及び特性解析について」等を参考とすること。ただし，より上流の過程で評価されていることに起因する正当な理由により検討事項の一部を省略することは差し支えない。

(5) 製造工程中の取り違え及びクロスコンタミネーション防止対策

ヒトES細胞由来分化細胞株からのヒトES細胞加工医薬品等の製造にあたっては，製造工程中の取り違え及びクロスコンタミネーションの防止が重要であり，工程管理における防止対策を明らかにすること。

3　最終製品の構成要素となる細胞の特性解析

最終製品の構成要素となる細胞については，例えば，未分化細胞の混入や目的外の細胞の混入を規定するための細胞純度をはじめとして，細胞生存率，形態学的特徴，細胞増殖特性，生化学的指標，免疫学的指標，特徴的産生物質，核型，分化能その他適切な遺伝型又は表現型の指標を解析するとともに，必要に応じて機能解析を行うこと。また，培養期間の妥当性及び細胞の安定性を評価するために，予定の培養期間を超えて培養した細胞において目的外の変化がないことを適切な細胞特性指標を用いて示すこと。これらの検討に際しては，あらかじめ試験的検体を用いた検討によって実施・検証しておくことでも良いが，これらの検討結果から患者に製品を適用する際に選択すべき重要細胞特性指標を明らかにしておくこと［注：特異的マーカーに加えて，網羅的解析，例えば1)CGHゲノム，2)エピジェネティックス（DNAメチル化），3) RNA，4) 糖鎖に関してアレイやチップ等を用いた解析が有用な場合もあるが，検体の量的制限や技術的限界もあり，可能な範囲で考慮すればよい］。適用後に体内での増殖等を期待する場合には，設定された基準による継代数又は分裂回数で期待された機能を発揮することを明らかにすること。

4　最終製品の形態，包装

最終製品の形態，包装は，製品の品質を確保できるものでなければならない。

5　製造方法の恒常性

ヒトES細胞加工医薬品等の製造に当たっては，製造工程を通じて，個別に加工した製品の細胞数，細胞生存率並びに製品の使用目的及び適用方法等からみた特徴（表現型の適切な指標，遺伝型の適切な指標，機能特性及び目的とする細胞の含有率等）が製品（ロット）間で本質的に損なわれないことを，試験的検体を用いてあらかじめ評価しておくこと。中間製品で評価することが，原材料としての細胞・組織の適格性や中間製品までの製造過程の妥当性をよく反映し，また，最終製品に向けての適正な道標となるなど，合理的な場合もあるので，必要に応じて選択肢とすること。

製造工程中の凍結保存期間や加工に伴う細胞培養の期間が長期に及ぶ場合には一定期間ごとに無菌試験を行うなど，無菌性が確保されることを確認すること。

6　製造方法の変更

開発途中に製造方法を変更した場合，変更前の製造方法による製品を用いて得た試験成績を確認申請又は承認申請に使用するときは，製造方法変更前後の製品の同等性／同質性を示すこと。

第3　最終製品の品質管理

1　総論

ヒトES細胞加工医薬品等の品質管理全体の方策としては，最終製品の規格及び試験方法の設定，個別患者への適用ごとの原材料の品質管理，製造工程の妥当性の検証と一定性の維持管理のほか，中間製品の品質管理を適正に行うこと等が挙げられる。

ヒトES細胞加工医薬品等においては目的細胞以外の未分化細胞の混入を否定するための方策が最も重要な要件の一つである。可能な限り中間製品の段階で目的細胞以外の未分化細胞の混入を否定することが望ましい。

最終製品の規格及び試験方法については，対象とする細胞・組織の種類及び性質，製造方法，各製品の臨床使用目的や使用方法，安定性，利用可能な試験法等によって異なると考えられるため，取り扱う細胞・組織によってこれらの違いを十分に考慮して設定すること。また，製造工程の妥当性の検証と一定性の維持管理法，中間製品の品質管理等との相互補完関係を考慮に入れて，全体として品質管理の目的が達成されるとの観点から，合理的に規格及び試験方法を設定し，その根拠を示すこと。なお，確認申請は，治験を実施する製品の品質として問題がないとみなせることを確認することを目的としている。したがって，無菌性やマイコプラズマの否

定など必須なものを除き，治験後に臨床試験成績と品質の関係を論ずるために必要な品質特性については，やむを得ない場合は少数の試験的検体の実測値をもとにその変動をしかるべき範囲内に設定する暫定的な規格及び試験方法を設定することで差し支えない。ただし，規格及び試験方法を含む品質管理法は治験の進行とともに充実・整備を図ること。

2　最終製品の品質管理法

最終製品について，以下に示す一般的な品質管理項目及び試験を参考として，必要で適切な規格及び試験方法を設定し，その根拠を明らかにすること。

ロットを構成しない製品を製造する場合は個別製品ごとに，ロットを構成する製品を製造する場合には，通常，各個別製品ではなく各ロットが品質管理の対象となるので，これを踏まえてそれぞれ適切な規格，試験方法を設定すること。

(1) 細胞数並びに生存率

得られた細胞の数と生存率は，最終製品又は必要に応じて適切な製造工程の製品で測定すること。なお，確認申請時においては，少数の試験的検体での実測値を踏まえた暫定的な規格を設定することでも良い。

(2) 確認試験

目的とする細胞・組織の形態学的特徴，生化学的指標，免疫学的指標，特徴的産生物質その他適切な遺伝型あるいは表現型のうち，重要細胞特性指標を選択して，目的とする細胞であることを確認すること。

(3) 細胞の純度試験

目的細胞以外の未分化細胞，異常増殖細胞，形質転換細胞の有無や混入細胞の有無等の細胞の純度について，目的とする細胞・組織の由来，培養条件等の製造工程，中間製品の品質管理等を勘案し，必要に応じて試験項目，試験方法及び判定基準を示すこと。なお，確認申請時においては，少数の試験的検体での実測値を踏まえた暫定的な規格を設定することでも良い。

(4) 細胞由来の目的外生理活性物質に関する試験

細胞由来の各種目的外生理活性物質のうち，製品中での存在量如何で患者に安全性上の重大な影響を及ぼす可能性が明らかに想定される場合には，適切な許容量限度試験を設定すること。なお，確認申請時においては，少数の試験的検体での実測値を踏まえた暫定的な規格を設定することでも良い。

(5) 製造工程由来不純物試験

原材料に存在するか又は製造過程で非細胞成分，培地成分（フィーダー細胞を含む），資材，試薬等に由来し，製品中に混入物，残留物，又は新たな生成物，分解物等として存在する可能性があるもので，かつ，品質及び安全性の面からみて望ましくない物質等（例えば，ウシ胎児血清由来のアルブミン，抗生物質等）については，当該物質の除去に関するプロセス評価や当該物質に対する工程内管理試験の結果を考慮してその存在を否定するか，又は適切な試験を設定して存在許容量を規定すること。試験対象物質の選定及び規格値の設定に当たっては，設定の妥当性について明らかにすること。

なお，確認申請時においては，少数の試験的検体での実測値を踏まえた暫定的な規格を設定することでも良い。

(6) 無菌試験及びマイコプラズマ否定試験

最終製品の無菌性については，あらかじめモデル検体を用いて全製造工程を通じて無菌性を確保できることを十分に評価しておく必要がある。最終製品について，患者に適用する前に無菌性（一般細菌及び真菌否定）を試験により示すこと。また，適切なマイコプラズマ否定試験を実施すること。検証された核酸増幅法を用いることでもよい。最終製品の無菌試験等の結果が，患者への投与後にしか得られない場合には，投与後に無菌性等が否定された場合の対処方法をあらかじめ設定しておくこと。また，この場合，中間製品で無菌性を試験により示し，最終製品に至る工程の無菌性を厳密に管理する必要がある。また，同一施設・同一工程で以前に他の患者への適用例がある場合には，全例において試験により無菌性が確認されていること。ロットを構成する製品で密封性が保証されている場合には，代表例による試験でよい。適用ごとに試験を実施する必要がある場合で，無菌試験等の結果が，患者への投与後にしか得られない場合には，適用の可否は直近のデータを参考にすることになるが，この場合でも最終製品の無菌試験等は必ず行うこと。

抗生物質は細胞培養系で極力使用しないことが望まれるが，使用した場合には，無菌試験に影響を及ぼさないよう処置すること。

(7) エンドトキシン試験

試料中の夾雑物の影響を考慮して試験を実施すること。規格値は必ずしも実測値によらず，日本薬局方等で示されている最終製品の1回投与量を基にした安全域を考慮して設定すればよい。また，工程内管理試験として設定することも考えられるが，その場合には，バリデーションの結果を含めて基準等を設定し，その妥当性を説明すること。

(8) ウイルス等の試験

製造工程中で生物由来成分を使用する場合には，最終製品で当該成分由来のウイルスについての否定試験の実施を考慮すべき場合もあるかも知れない。しかし可能な限り，もとの成分段階での試験やプロセス評価で迷入が否定されているこ

とが望ましい。

(9) 効能試験

細胞種，臨床使用目的又は特性等に応じた適切な効能試験の実施を考慮すべき場合もある。なお，確認申請においては，少数の試験的検体による実測値を踏まえた暫定的な規格を設定することでも良い。

(10) 力価試験

細胞・組織から分泌される特定の生理活性物質の分泌が当該ヒトES細胞加工医薬品等の効能又は効果の本質である場合には，その目的としている必要な効果を発揮することを示すために，当該生理活性物質に関する検査項目及び規格を設定すること。遺伝子を導入した場合の発現産物又は細胞から分泌される目的の生成物等について，力価，産生量等の規格を設定すること。なお，確認申請時においては，少数の試験的検体による実測値を踏まえた暫定的な規格を設定することでも良い。

(11) 力学的適合性試験

一定の力学的強度を必要とする製品については，適用部位を考慮した力学的適合性及び耐久性を確認するための規格を設定すること。なお，確認申請時においては，少数の試験的検体による実測値を踏まえた暫定的な規格を設定することでも良い。

第3章　ヒトES細胞加工医薬品等の安定性

製品化したヒトES細胞加工医薬品等又は重要なそれらの中間製品について，保存・流通期間及び保存形態を十分考慮して，細胞の生存率及び力価等に基づく適切な安定性試験を実施し，貯法及び有効期限を設定し，その妥当性を明らかにすること。特に凍結保管及び解凍を行う場合には，凍結及び解凍操作による製品の安定性や規格への影響がないかを確認すること。また，必要に応じて標準的な製造期間を超える場合や標準的な保存期間を超える長期保存についても検討し，安定性の限界を可能な範囲で確認すること。ただし，製品化後直ちに使用するような場合はこの限りではない。

また，製品化したヒトES細胞加工医薬品等を運搬する場合には，運搬容器及び運搬手順(温度管理等を含む)等を定め，その妥当性について明らかにすること。

第4章　ヒトES細胞加工医薬品等の非臨床安全性試験

製品の特性及び適用法から評価が必要と考えられる安全性関連事項について，技術的に可能であれば，科学的合理性のある範囲で，適切な動物を用いた試験又は *in vitro* での試験を実施すること。なお，非細胞成分及び製造工程由来の不純物等については，可能な限り，動物を用いた試験ではなく理化学的分析法により評価すること。また，最終製品における未分化細胞の存在が異所性組織形成や腫瘍形成・がん化の可能性など安全性上の重要な関心事であるが，可能な限り，セル・バンクや中間製品段階等での徹底的な解析により，混在の可能性を否定するか，あるいは，目的細胞から未分化細胞の効果的分離・除去法や不活化法を開発し，活用することにより，混在の可能性を最小限にする努力が求められる。さらに，投与経路等の選択も安全性上の懸念を最小限にするための有用な方策であるかも知れない。

ヒト由来の製品を実験動物等で試験して必ずしも意義ある結果が得られるとは限らない。このため，動物由来の製品モデルを作製し適切な実験動物に適用する試験系により試験を行うことで，より有用な知見が得られると考えられる場合には，むしろ，このような試験系を用いることに科学的合理性がある場合があるかも知れない。その際は，対象製品及び対象疾患ごとに適切な中・大動物を用いた試験の実施を積極的に考慮する(注：例えば神経疾患ならばサル等，循環器疾患ならばブタ・イヌ等が適している場合がある)。ただし，ヒトiPS(様)細胞加工医薬品等を構成する細胞と同一の特徴を有する細胞集団が同一の手法にてヒト以外の動物種からも得られるとは限らず，また同様の培養条件等で同等／同質な製品が製造できるとも限らないことから，このような試験の採用，実施及び評価にあたっては，慎重な事前検討や対応が必要である。ヒト以外の動物種から得たES細胞細胞加工製品を用いて動物実験を行った場合，その外挿可能性を説明すること。場合によっては細胞を用いる試験系も考慮し，このようなアプローチにより試験を行なった際には，その試験系の妥当性について明らかにすること。

以下に，必要に応じて非臨床的に安全性を確認する際の参考にすべき事項及び留意点の例を示す。これらは例示であって，合理性のない試験の実施を求める趣旨ではなく，製品の特性及び臨床適用法等を考慮して，必要かつ適切な試験を実施し，その結果について総合的な観点から評価，考察すること。

1　培養期間を超えて培養した細胞について，目的外の形質転換を起こしていないことや目的細胞以外の細胞が異常増殖していないことを明らかにすること。

2　必要に応じて細胞・組織が産生する各種サイトカイン，成長因子等の生理活性物質の定量を行い，生体内へ適用したときの影響に関して考察を行うこと。

3　製品の適用が患者の正常な細胞又は組織に影響を与える可能性，及びその安全性について検討，考察すること。

4　患者への適用により，製品中の細胞や混入する未分化細胞が異所性組織を形成する可能性，及びその安全性について検討，考察すること。その際，製品の種類や特性，投与経路，

対象疾患，及び試験系の妥当性等を総合的に勘案すること。
5　製品及び導入遺伝子の発現産物等による望ましくない免疫反応が生じる可能性，及びその安全性について検討，考察すること。
6　最終製品の細胞または中間製品の細胞について，適切な動物モデル等を利用し，良性腫瘍を含む腫瘍形成及びがん化の可能性に関して検討，考察すること。その際，製品の種類や特性，投与量・投与経路，対象疾患，及び試験系の妥当性等を総合的に勘案すること。また，腫瘍形成またはがん化の可能性がある場合には，期待される有効性との関係等を勘案して，使用することの妥当性及び合理性について明らかにすること。
（注：造腫瘍性試験において最も重要なのは，最終製品が患者に適用された場合の製品の造腫瘍性を的確に評価することである。しかし，十分な細胞数が得られない等の理由により最終製品を構成する細胞を用いることができず，中間製品の細胞を用いて最終製品の造腫瘍性を評価しなければならない場合も想定される。また，動物モデルを使用した造腫瘍性試験においては，細胞の分散や足場への接着，細胞密度，投与部位等の条件が最終製品と必ずしも一致するものではない。さらに，動物の種・系統・免疫状態による感度差もある。これらの事情を総合的に勘案して，最終製品の造腫瘍性を評価する必要がある。また，最終製品の造腫瘍性に起因する患者へのリスクについては，対象疾患を治療することによる患者へのベネフィット等とのバランスを踏まえて合理的に評価すること。）
7　製造工程で外来遺伝子の導入が行われ，最終製品中で機能している場合や残存している場合には，遺伝子治療用医薬品指針に定めるところに準じて試験を行うこと。特に，ウイルスベクターを使用した場合には増殖性ウイルスがどの程度存在するかを検査するとともに，検査方法が適切であることについても明らかにすること。
　また，導入遺伝子及びその産物の性状について調査し，安全性について明らかにすること。細胞については，増殖性の変化，良性腫瘍を含む腫瘍形成及びがん化の可能性について考察し，明らかにすること。
8　動物由来のモデル製品を含めて製品の入手が容易であり，かつ臨床上の適用に関連する有用な安全性情報が得られる可能性がある場合には，合理的に設計された一般毒性試験の実施を考慮すること。
　なお，一般毒性試験の実施に当たっては，平成元年9月11日付け薬審1第24号厚生省薬務局新医薬品課長・審査課長連名通知「医薬品の製造（輸入）承認申請に必要な毒性試験のガイドラインについて」の別添「医薬品毒性試験法ガイドライン」等を参照すること。

第5章　ヒトES細胞加工医薬品等の効力又は性能を裏付ける試験

1　技術的に可能かつ科学的に合理性のある範囲で，実験動物又は細胞等を用い，適切に設計された試験により，ヒトES細胞加工医薬品等の機能発現，作用持続性及び医薬品・医療機器として期待される臨床効果の実現可能性（Proof-of-Concept）を示すこと。
2　遺伝子導入細胞にあっては，導入遺伝子からの目的産物の発現効率及び発現の持続性，導入遺伝子の発現産物の生物活性並びに医薬品等として期待される臨床効果の実現可能性（Proof-of-Concept）を示すこと。
3　適当な動物由来細胞・組織製品モデル又は疾患モデル動物がある場合には，それを用いて治療効果を検討すること。
4　確認申請段階では，当該製品の効力又は性能による治療が他の治療法と比較したときはるかに優れて期待できることが国内外の文献又は知見等により合理的に明らかにされている場合には，必ずしも詳細な実験的検討は必要とされない。

第6章　ヒトES細胞加工医薬品等の体内動態

1　製品を構成する細胞・組織及び導入遺伝子の発現産物について，技術的に可能で，かつ，科学的合理性がある範囲で，実験動物での吸収及び分布等の体内動態に関する試験等により，患者等に適用された製品中の細胞・組織の生存期間，効果持続期間を推測し，目的とする効果が十分得られることを明らかにすること［注：体内動態に関する試験等には，例えば組織学的検討，磁気共鳴画像診断法（MRI），陽電子放射断層撮影法（PET），単一光子放射断層撮影法（SPECT），光イメージングなどがある。］
2　ヒトES細胞加工医薬品等の用法（投与方法）について，動物実験を通してその合理性を明らかとすること。特に，全身投与にあっては投与後の細胞の全身分布を動物実験などから外挿し，有用性の観点から議論すること。［注：投与経路ごとにどこに生着するかは不明であるが，全身投与よりも局所投与が望ましいと想定される。しかし，全身投与であってもその有用性において被投与患者に有益であると合理的に説明が可能である場合には用法として設定可能である。例えば，あるES細胞加工医薬品等を肝疾患治療剤として肝臓への生着を期待する場合，肝臓へ効率よく到達させかつその他の臓器への分布を最低限に抑えることが合理的な投与方法であると想定されるが，経末梢静脈投与により当該細胞が肝臓に集積し，他臓器に生着しないことが証明できれば良い。しかし，異所性生着しても，被投与患者にとって不利益（生体機能への悪影響）が生じない場合は用法として肯定できるかも知れない。異所性分化による不利益とは，例えば当該細胞が心臓に異所性生着して骨形成する場合が想定され，それが不整脈

を意起したような場合である。]

3　当該細胞・組織が特定の部位(組織等)に直接適用又は到達して作用する場合には，その局在性を明らかにし，局在性が製品の有効性・安全性に及ぼす影響を考察すること。

第7章　臨床試験

ヒトES細胞加工医薬品等の治験を開始する(First-in-Man)に当たって支障となる品質及び安全性上の問題が存在するか否かの確認申請の段階においては，臨床上の有用性を勘案して評価されるものであり，ヒトES細胞加工医薬品等について予定されている国内の治験計画について以下の項目を踏まえて評価すること。その際，明らかに想定される製品のリスクを現在の学問・技術を駆使して排除し，その科学的妥当性を明らかにした上で，なお残る未知のリスクと，重篤で生命を脅かす疾患，身体の機能を著しく損なう疾患，身体の機能や形態を一定程度損なうことによりQOLを著しく損なう疾患などに罹患し，従来の治療法では限界があり，克服できない患者が新たな治療機会を失うことにより被るかも知れないリスクとのリスクの大小を勘案し，かつ，これらすべての情報を開示した上で患者の自己決定権に委ねるという視点を導入することが望まれる。

1　対象疾患

2　対象とする被験者及び被験者から除外すべき患者の考え方

3　ヒトES細胞加工医薬品等及び併用薬の適用を含め，被験者に対して行われる治療内容(注：投与・移植した細胞の機能を維持・向上・発揮させるために併用する薬剤が想定される場合，当該薬剤の作用を *in vitro* あるいは *in vivo* で検証すること)

4　既存の治療法との比較を踏まえた臨床試験実施の妥当性

5　現在得られている情報から想定される製品及び患者のリスク及びベネフィットを含め，被験者への説明事項の案

なお，臨床試験は，適切な試験デザイン及びエンドポイントを設定して実施する必要があり，目的とする細胞・組織の由来，対象疾患及び適用方法等を踏まえて適切に計画すること。

OPEN ACCESS Freely available online

PLoS one

Defining Hypo-Methylated Regions of Stem Cell-Specific Promoters in Human iPS Cells Derived from Extra-Embryonic Amnions and Lung Fibroblasts

Koichiro Nishino[1], Masashi Toyoda[1], Mayu Yamazaki-Inoue[1], Hatsune Makino[1], Yoshihiro Fukawatase[1], Emi Chikazawa[1], Yoriko Takahashi[1], Yoshitaka Miyagawa[2], Hajime Okita[2], Nobutaka Kiyokawa[2], Hidenori Akutsu[1], Akihiro Umezawa[1]*

1 Department of Reproductive Biology, National Institute for Child Health and Development, Tokyo, Japan, **2** Department of Developmental Biology, National Institute for Child Health and Development, Tokyo, Japan

Abstract

Background: Human induced pluripotent stem (iPS) cells are currently used as powerful resources in regenerative medicine. During very early developmental stages, DNA methylation decreases to an overall low level at the blastocyst stage, from which embryonic stem cells are derived.Therefore, pluripotent stem cells, such as ES and iPS cells, are considered to have hypo-methylated status compared to differentiated cells. However, epigenetic mechanisms of "stemness" remain unknown in iPS cells derived from extra-embryonic and embryonic cells.

Methodology/Principal Findings: We examined genome-wide DNA methylation (24,949 CpG sites covering 1,3862 genes, mostly selected from promoter regions) with six human iPS cell lines derived from human amniotic cells and fetal lung fibroblasts as well as two human ES cell lines, and eight human differentiated cell lines using Illumina's Infinium HumanMethylation27. A considerable fraction (807 sites) exhibited a distinct difference in the methylation level between the iPS/ES cells and differentiated cells, with 87.6% hyper-methylation seen in iPS/ES cells. However, a limited fraction of CpG sites with hypo-methylation was found in promoters of genes encoding transcription factors. Thus, a group of genes becomes active through a decrease of methylation in their promoters. Twenty-three genes including *SOX15*, *SALL4*, *TDGF1*, *PPP1R16B* and *SOX10* as well as *POU5F1* were defined as genes with hypo-methylated SS-DMR (Stem cell-Specific Differentially Methylated Region) and highly expression in iPS/ES cells.

Conclusions/Significance: We show that DNA methylation profile of human amniotic iPS cells as well as fibroblast iPS cells, and defined the SS-DMRs. Knowledge of epigenetic information across iPS cells derived from different cell types can be used as a signature for "stemness" and may allow us to screen for optimum iPS/ES cells and to validate and monitor iPS/ES cell derivatives for human therapeutic applications.

Citation: Nishino K, Toyoda M, Yamazaki-Inoue M, Makino H, Fukawatase Y, et al. (2010) Defining Hypo-Methylated Regions of Stem Cell-Specific Promoters in Human iPS Cells Derived from Extra-Embryonic Amnions and Lung Fibroblasts. PLoS ONE 5(9): e13017. doi:10.1371/journal.pone.0013017

Editor: Tadafumi Kato, RIKEN Brain Science Institution, Japan

Received April 21, 2010; **Accepted** September 6, 2010; **Published** September 27, 2010

Funding: This study was supported by grants from the Ministry of Education, Culture, Sports, Science, and Technology (MEXT) of Japan; Ministry of Health, Labour and Welfare Sciences (MHLW) research grants; by a Research Grant on Health Science focusing on Drug Innovation from the Japan Health Science Foundation; by the program for the promotion of Fundamental Studies in Health Science of the Pharmaceuticals and Medical Devices Agency; by a Research Grant for Cardiovascular Disease from the MHLW; and by a Grant for Child Health and Development from the MHLW. The funders had no role in study design, data collection and analysis, decision to publish, or preparation of the manuscript.

Competing Interests: The authors have declared that no competing interests exist.

* E-mail: umezawa@1985.jukuin.keio.ac.jp

Introduction

Human embryonic stem (ES) cells [1] and induced pluripotent stem (iPS) cells [2,3,4,5] are currently used as powerful resources in regenerative medicine. However, epigenetic mechanisms of "stemness" remain unknown. DNA methylation is known to be a key component in normal differentiation and development [6,7]. Tissue-specific genes, such as *OCT-4/3* [8], *Sry* (sex determining region on Y chromosome) [9] and *MyoD* [10], show tissue-specific demethylation corresponding to their expression during development. Furthermore, DNA methylation in cells specifically varies depending on cell lineage and tissue types [7]. Transformation to iPS cells from differentiated cells requires a process of epigenetic reprogramming [11]. Understanding the epigenetic regulation in human pluripotent stem cells, therefore, enable us to elucidate "stemness" and to screen for optimum iPS/ES cells for human therapeutic applications. Human extra-embryonic amnion cells are a useful cell source for generation of iPS cells, because they can be collected without invasion and are conventionally freeze-storable. Recently, we generated iPS cells from human amnion cells as well as human fetal lung fibroblast cells [12,13]. Here, we show DNA methylation profiles of human pluripotent stem cells including iPS cells, which were derived from extra-embryonic amnion cells and fetal lung fibroblast cells, and human ES cells. We also defined another subset that may play a key practical role in maintaining the state of "stemness".

Results

Analysis of genome-wide DNA methylation

Human iPS cell lines (MRC-iPS [13] and AM-iPS cell lines [12]) independently established in our laboratory by retroviral infection of 4 genes (*OCT-3/4*, *SOX2*, *c-MYC*, and *KLF4*), based on the Yamanaka's pioneer protocols [2] from 2 fully differentiated cells (MRC-5, fetal lung fibroblast cells, and AM936EP, amnion cells), were used as a primary source for experimentation (Table 1). These cells clearly showed human iPS characters [12,13].

To examine DNA methylation status in six iPS, two ES [14], and eight differentiated cell lines (Table 1), we therefore examined genome-wide DNA methylation using Illumina's Infinium HumanMethylation27 BeadChip, on which oligonucleotides for 27,578 CpG sites covering more than 14,000 genes are mounted, mostly selected from promoter regions. This assay system provides advantageous quantitative measurement. DNA methylation levels were recorded using a scoring system ranging from "0" (completely unmethylated) to "1" (fully-methylated). Using multiple repetitions, we analyzed 24,949 out of 27,578 CpG sites with 16 samples (see Materials and Methods), categorizing them into three groups; Low (score$\leq$0.3), Middle (0.3<score$\leq$0.7), or High (0.7<score) methylation. Overall, methylation levels in pluripotent stem cells and differentiated cells are shown in Fig. 1A, with the levels in each cell line presented in Table S1. While the percentage of the High class in differentiated cells was 16.3% on average, the percentage in iPS/ES cells was 25.3% (Fig. 1A). The number of CpG sites categorized in the High class is significantly greater in pluripotent stem cells compared with differentiated cells. Hierarchical clustering analysis clearly discriminates iPS/ES cells from the differentiated cells (Fig. 1B). Hyper-methylated sites (shown in red) are widespread in the heat map in iPS/ES cells, compared with the differentiated cells (Fig. 1B), suggesting that gene promoters in iPS/ES cells are hyper-methylated, compared with those in differentiated cells.

About two-thirds of the CpG sites were at a Low methylated level in both iPS/ES cell and differentiated cell groups (Fig. 1A and B). Another computation found 13,971 CpG sites to consistently show a score of lower than 0.3. This suggests that a significant fraction of the CpG sites examined may have less involvement in methylation, although some might become methylated under different conditions. As most CpG sites on the chip were chosen simply based on the location in promoters, it is possible that some CpG sites may be positioned at a distance from the target site, even in a promoter controlled by DNA methylation. Analysis of our and all published data indicated that a group of CpG sites more suitable to methylation analyses could be identified, allowing us to focus attention on specific changes in methylation levels seen between iPS/ES and differentiated cells.

Differentially methylated site (DMS) in the promoters. Firstly, we defined the "differentially methylated site" (DMS), representing a CpG site whose score differed 0.3 points and more between the two cell groups. The DMSs between MRC-iPS and AM-iPS cells, and also between iPS and ES cells, were only 1.0% and 2.8% of all the CpG sites, respectively (Fig. 1C), suggesting that iPS and ES cells have similar methylation status. In contrast, the DMSs between AM936EP and AM-iPS cells, and between MRC-5 and MRC-iPS cells, were 11.3% and 10.6%, respectively, suggesting that iPS cells and their parental cells have differentially methylated status (Fig. 1C and D). It should be noted that approximately 80% of the DMSs between the iPS cells and their parental cells changed to a "hyper-methylated" state from a "hypo-methylated" state in iPS cells (Fig. 1C). Comparison of DMSs between AM- and MRC-iPS cells, and between iPS and ES cells show slight but significant difference (Fig. 1C). In 261 DMSs between MRC- and AM-iPS cells (MA-DMSs), 203 sites in AM-iPS cells and 165 in MRC-iPS cells showed no difference from their parental cells, suggesting that these sites in iPS cells are inherited from their tissue origin (Fig. 1E). In addition, 414 out of 694 DMSs between MRC-iPS and ES cells (ME-DMSs) and 581 out of 990 DMSs between AM-iPS and ES cells (AE-DMSs) are inherited DMSs (Fig. 1E). Interestingly, approximately 40% of DMSs between iPS and ES cells are iPS-specific DMSs, meaning that these sites are aberrant methylated in iPS cells (Fig. 1E). In

Table 1. A list of human cells analyzed for a methylation state in this study.

Cell ID	Description	ability of differentiation
MRC5	Fetal lung fibroblast cells	None
MRC-iPS-11	MRC5-derived iPS cells (P4)	Pluripotent
MRC-iPS-19	MRC5-derived iPS cells (P4)	Pluripotent
MRC-iPS-75	MRC5-derived iPS cells (P4)	Pluripotent
AM936EP	Amnion-derived cells (P6)	None
AM-iPS-3	AM936EP -derived iPS cells (P4)	Pluripotent
AM-iPS-6	AM936EP -derived iPS cells (P4)	Pluripotent
AM-iPS-8	AM936EP -derived iPS cells (P4)	Pluripotent
UtE1104	Endometrium-derived cells (P7)	None
H4-1	Bone marrow stroma-derived cells (P26)	None
Mim1508E	Auricular cartilage-derived cells (P1)	Cartilage
Yub636BM	Extra finger bone marrow-derived cells (P3)	Bone
PAE551	Placental artery endothelial cells (P13)	None
Edom22	Menstrual blood-derived cells (P1)	Myoblast
HUES3	Embryonic stem cells (P29)	Pluripotent
HUES8	Embryonic stem cells (P24)	Pluripotent

Numbers in parenthesis with P indicate passage in culture on the cells used in the methylation analysis.
doi:10.1371/journal.pone.0013017.t001

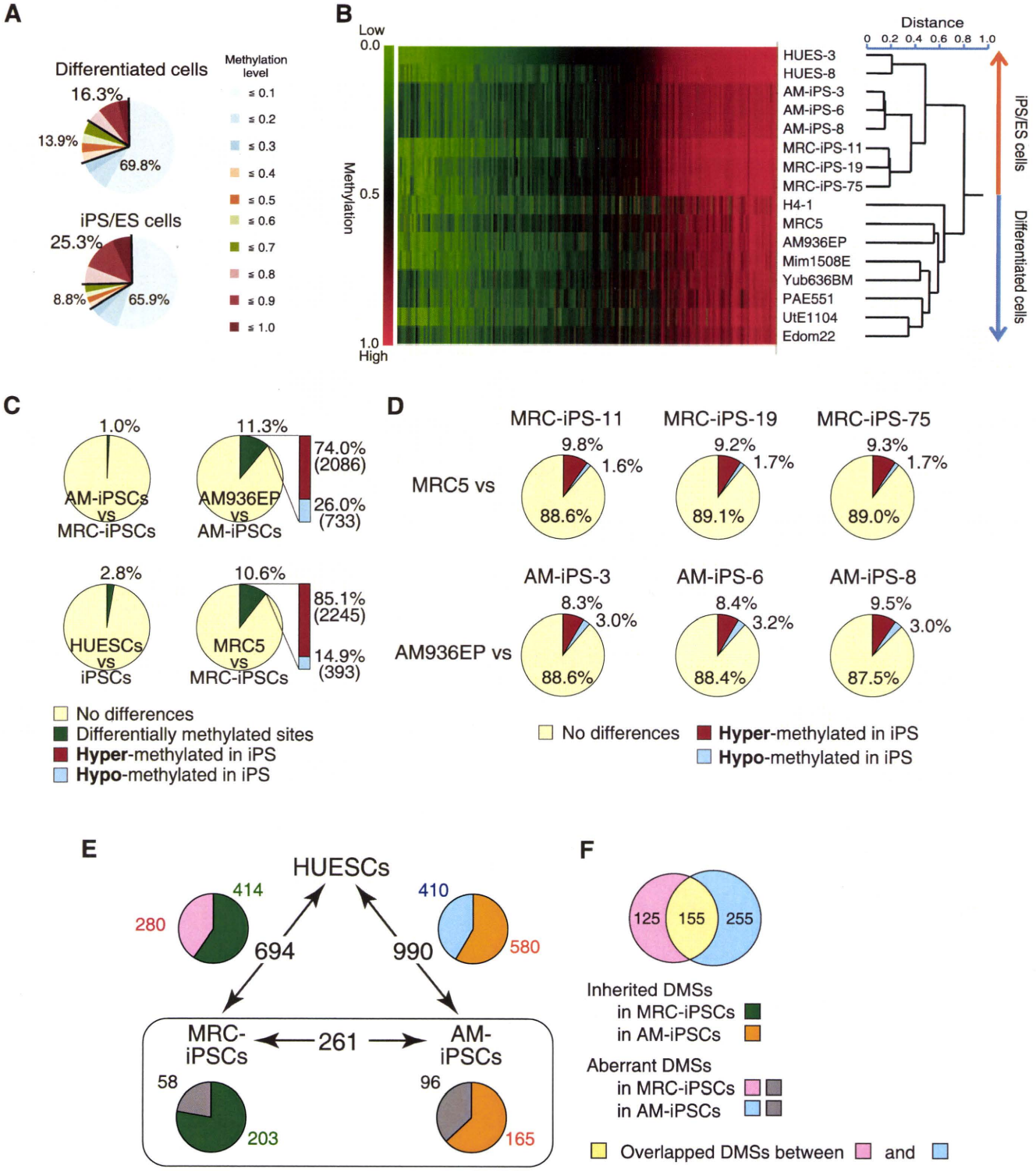

Figure 1. The ratio of hyper-methylated sites in iPS/ES cells was significantly larger than that of the differentiated cells. (**A**) Ratio of Low (methylation score≤0.3), Middle (0.3<score≤0.7), and High (0.7<score) methylated states in 24,949 CpG sites. (**B**) Clustering analysis. Heat map showing hyper-methylation in human iPS/ES cells compared with differentiated cells. The Heat map in hierarchical clustering analysis represented DNA methylation levels from completely methylated (red) to unmethylated (green). Epigenetic distances (Euclidean Distance) were calculated by NIA Array. (**C**) Comparisons of CpG sites between two groups show high similarities between AM-iPS and MRC-iPS cells or between human ES cells (HUESCs) and iPS cells (iPSCs). In contrast, 11.3% and 10.6% of CpG sites are differentially methylated in AM-iPS and MRC-iPS cells, respectively, compared to their parental cells (AM936EP and MRC5). It should be noted that 74.0% and 85.1% of the differentially methylated sites (DMSs) are hyper-methylated in AM-iPS and MRC-iPS cells, respectively, compared to their parental cells. (**D**) Comparison of the 24,949 CpG sites between iPS cells and their parental cells. (**E**) DMSs among human ES cells, AM- and MRC-iPS cells. The relative amount of inherited/aberrant DMSs is indicated in the pie chart. (**F**) Overlapped aberrant DMSs between MRC- and AM-iPS cells.
doi:10.1371/journal.pone.0013017.g001

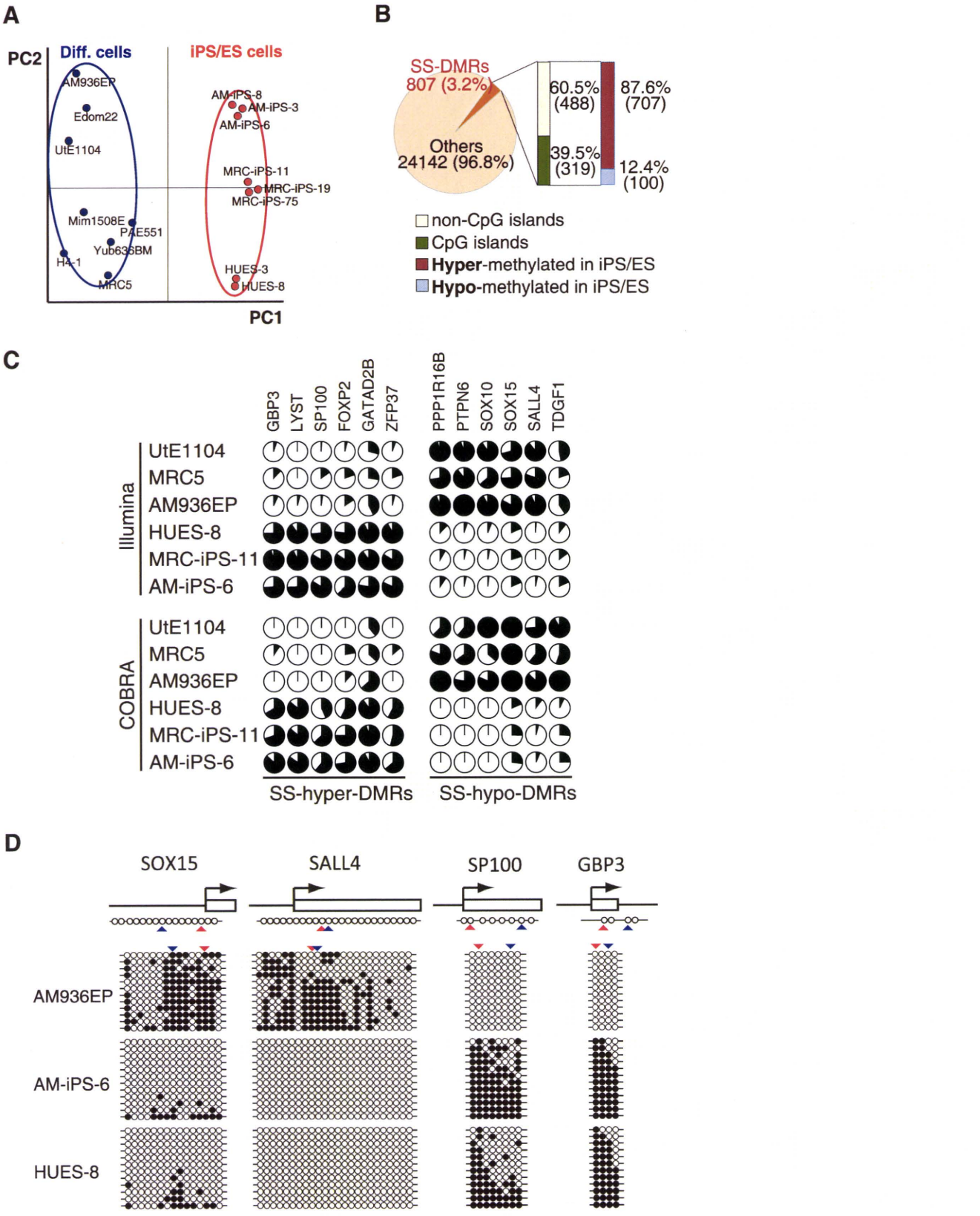

Figure 2. Pluripotent stem cells are significantly more hyper-methylated than differentiated cells. (**A**) Principal component analysis (PCA) for DNA methylation states of 24,949 CpG sites with 16 human cell lines. The PC1 axis clearly distinguish iPS/ES cell group from differentiated cells, while human iPS cells are very close to human ES cells. (**B**) Stem cell-specific differently methylated regions (SS-DMRs) were defined by PC1. In the pluripotent stem cells, 60.5% of the SS-DMRs are located outside of CpG islands and 87.6% of the SS-DMRs are hyper-methylated. (**C**) DNA methylation levels at promoter regions in 12 representative genes determined by Illumina Infinium HumanMethylation27 assay and Bio-COBRA.

Details of these genes are described in Table S6B. The promoter regions of these genes were defined as the SS-DMRs. The relative amount of methylated DNA ratio is indicated as the black area in the pie chart. The same methylation patterns in 12 regions were detected both by Infinium assay and COBRA. (**D**) Bisulfite sequencing analysis of the same regions that were analyzed by Infinium assay and COBRA assay in *SOX15*, *SALL4*, *SP100* and *GBP3*. (Top) Schematic diagram of the genes. Arrows, open boxes and open circles represent transcription start site, first exon and position of CpG sites, respectively. (Bottom) Open and closed circles indicate unmethylated and methylated states, respectively. Red and blue arrowheads represent the position of CpG sites in Infinium assay and COBRA, respectively.
doi:10.1371/journal.pone.0013017.g002

aberrant DMSs, 155 sites overlapped between MRC- and AM-iPS cells (Fig. 1F and data set S1, S2, S3). Overlapping aberrant DMSs are located at promoters in genes such as gene for FZD10, MMP9 and three zinc finger proteins (ZNF551, ZNF513 and ZNF540). These genes are hyper-methylated in iPS cells than parental cells and ES cells. Approximately 80% of aberrant DMSs are hyper-methylated, compared with parent cells and ES cells.

Defining stem cell specific differentially methylated regions (SS-DMRs). Principal component analysis (PCA) shows high similarity among human iPS and ES cells and clearly separates the iPS/ES cells from the differentiated cells, which is supported by hierarchical clustering analysis (Fig. 1B and Fig. 2A). Based on principal component 1 (PC1), 807 (3.2%) out of 24,949 sites were deduced to change their methylation state along with "stemness" (Fig. 2B). We designated a region represented by such CpG sites as "stem cell specific differentially methylated regions" (SS-DMRs). Of the 807 SS-DMRs, 39.5% (319 sites) are localized on CpG islands, whereas 60.5% (488 sites) are not (Fig. 2B), although 72.5% CpG sites on the bead-chips occur on CpG islands. Thus, promoter regions on non-CpG islands were more affected during reprogramming towards pluripotent stem cells. 707 sites (87.6%) of the SS-DMRs were significantly increased in the methylation levels in iPS/ES cells, compared with those in the differentiated cells, and we designated these sites as "stem cell specific hyper-differentially methylated regions (SS-hyper-DMRs) " (Fig. 2B and data set S4). In contrast, 100 sites (12.4%) were decreased and designated as "stem cell specific hypo-differentially methylated regions (SS-hypo-DMRs) " (Fig. 2B and data set S5). We also confirmed the methylation state in the promoter regions for some of the detected genes by another means, i.e. quantitative combined bisulfite restriction analysis (COBRA) [15] (Fig. 2C). In addition, results of bisulfite sequencing of the region surrounding the SS-DMRs corresponded to results of Infinium assay and COBRA (Fig. 2D).

Gene ontology analysis with the SS-DMRs. We searched gene ontology databases for details of the SS-DMRs. Interestingly, SS-hypo-DMRs are abundant in genes related to nucleic acid binding and transcription factors, which may function in iPS cells. On the other hands, SS-hyper-DMRs are abundant in genes related to differentiation (Table 2). We also subjected the SS-DMRs to KEGG (Kyoto Encyclopedia of Genes and Genomes) pathway. Cytokine receptor interaction cascade, MAPK signaling, and Neuroactive ligand-receptor interaction are all major keywords for SS-hyper-DMRs (Table S2).

Expression of genes with SS-DMRs in human iPS/ES cells. To address whether changes in DNA methylation state are associated with expression levels, we surveyed genes showing more than 5-fold change of expression in human iPS/ES cells, compared with those in differentiated cells, using the GEO database [16,17]. Twenty-three genes represented by SS-hypo-DMRs were found in "genes significantly expressed in iPS/ES cells" (Table 3 and Table S3A). Representative genes, including *SOX15*, *SALL4*, *TDGF1*, *PPP1R16B* and *SOX10*, are expressed with hypo-methylation states in iPS/ES cells (Fig. 3A). On the other hand, forty-three genes represented by SS-hyper-DMRs were found in "genes significantly suppressed in iPS/ES cells" (Table S3B and S4). Representative genes, *SP100* and *GBP3*, are suppressed by hyper-methylation in iPS/ES cells (Fig. 3A). Among DNA methyltransferases, *DNMT3B* was reported to be highly expressed in human ES cells [18]. *DNMT3A*, *DNMT3B* and *DNMT3L* were indeed expressed in iPS/ES cells (Fig. 3A). The *DNMT3A* promoter in iPS/ES cells became demethylated, while *DNMT3B* and *DNMT3L* promoters remained low methylated during reprogramming (Fig. 3A and Table S5A), leading us to analyze chromatin in iPS/ES cells in addition to DNA methylation.

Histone H3K4 and H3K27 modification of genes with the SS-DMRs. Histone modification is another important mechanism in epigenetics. Methylation of lysine 4 (K4) and 27 (K27) on histone H3 is associated with active and silent gene expression, respectively [19], while bivalent trimethylation (me3) of H3K4 and K27 represses their gene expression in ES cells [20,21]. Based on the database of the UCSC Genome Bioinformatics, the promoter of *DNMT3B* in human ES cells is highly modified by 3K4me3, compared with that in human lung fibroblasts (Table S5B). No differences in histone modification of H3K4me3 or H3K27me3 between ES and lung fibroblasts at promoter of *DNMT3L* were detected (Table S5B). We also compared DNA methylation of the SS-DMRs with reported data for whole-genome mapping of H3K4me3 and H3K27me3 in the promoter regions of human ES cells [22]. In SS-hyper-DMRs, 68.8% do not have trimethylation of H3K4 and K27 (Fig. 3B). On the other hand, 42.3%, 1.3%, and 30.8% of SS-hypo-DMRs are marked with H3K4me3, H3K27me3, and bivalent H3K4me3 and K27me3, respectively (Fig. 3B). Thirteen out of the 23 genes in

Table 2. A list of top 7 categories of GO Term in "SS-DMRs".

Molecular Function		
PantherID: GO Term	**Count. Genes**	**%**
SS-hypo-DMRs		
MF00042:Nucleic acid binding	30	41.10%
MF00036:Transcription factor	15	20.55%
MF00099:Small GTPase	11	15.07%
MF00137:Glycosyltransferase	8	10.96%
MF00082:Transporter	6	8.22%
MF00154:Metalloprotease	6	8.22%
MF00098:Large G-protein	6	8.22%
SS-hyper-DMRs		
MF00213:Non-receptor serine/threonine protein kinase	124	20.98%
MF00262:Non-motor actin binding protein	119	20.14%
MF00001:Receptor	80	13.54%
MF00131:Transferase	76	12.86%
MF00099:Small GTPase	66	11.17%
MF00242:RNA helicase	57	9.64%
MF00261:Actin binding cytoskeletal protein	53	8.97%

doi:10.1371/journal.pone.0013017.t002

Table 3. A list of 23 genes with SS-hypo-DMRs exhibiting 'high' expression in human iPS/ES cells.

TargetID	Gene name	Fold change of expression	DNA methylation level in iPS/ES cells	DNA methylation level in Diff. cells
cg07337598	*ANXA9, annexin A9*	5.53	0.294±0.023	0.712±0.014
cg24183173	*BCOR, BCL-6 interacting corepressor*	5.06	0.014±0.005	0.784±0.051
cg21207436	*C14orf115, hypothetical protein LOC55237*	63.49	0.052±0.005	0.442±0.036
cg22892904	*CBX2, chromobox homolog 2*	11.48	0.068±0.006	0.607±0.051
cg24754277	*DAPK1, death-associated protein kinase 1*	28.34	0.115±0.005	0.708±0.049
cg21629895	*DNMT3A, DNA cytosine methyltransferase 3 alpha*	12.88	0.452±0.011	0.769±0.039
cg02932167	*ECEL1, endothelin converting enzyme-like 1*	17.57	0.115±0.007	0.672±0.059
cg25431974	*ECEL1, endothelin converting enzyme-like 1*	17.57	0.125±0.013	0.674±0.093
cg04515567	*FOXH1, forkhead box H1*	55.88	0.602±0.014	0.855±0.006
cg04464446	*GAL, galanin preproprotein*	194.63	0.241±0.022	0.735±0.056
cg00943909	*GNAS, guanine nucleotide binding protein*	47.33	0.076±0.016	0.528±0.081
cg27661264	*GNAS, guanine nucleotide binding protein*	47.33	0.037±0.005	0.355±0.054
cg18741908	*GPR160, G protein-coupled receptor 160*	60.48	0.068±0.006	0.466±0.038
cg20674521	*KCNJ4, potassium inwardly-rectifying channel J4*	6.11	0.306±0.024	0.772±0.043
cg21129531	*LRRC4, netrin-G1 ligand*	7.04	0.027±0.004	0.788±0.058
cg06144905	*PIPOX, L-pipecolic acid oxidase*	42.97	0.100±0.015	0.558±0.080
cg13083810	*POU5F1, POU domain; class 5;*	559.14	0.563±0.025	0.919±0.009
cg27377213	*PPP1R16B, protein phosphatase 1 regulatory inhibitor subunit 16B*	65.86	0.097±0.009	0.796±0.102
cg19580810	*RAB25, member RAS oncogene family*	6.16	0.062±0.010	0.703±0.030
cg09243900	*RAB25, member RAS oncogene family*	6.16	0.105±0.013	0.595±0.031
cg06303238	*SALL4, sal-like 4*	227.35	0.013±0.005	0.736±0.075
cg06614002	*SOX10, SRY-box 10*	5.23	0.028±0.005	0.829±0.046
cg01029592	*SOX15, SRY-box 15*	10.19	0.174±0.011	0.692±0.032
cg10242476	*TDGF1, teratocarcinoma-derived growth factor 1*	2472.59	0.146±0.013	0.387±0.052
cg20277416	*TM7SF2, transmembrane 7 superfamily member 2*	5.23	0.380±0.017	0.833±0.027
cg05656364	*VAMP8, vesicle-associated membrane protein 8*	9.69	0.070±0.010	0.698±0.081

Fold change of expression: Fold change of expression of the listed gene in human iPS/ES cells against the expression level in differentiated cells.

doi:10.1371/journal.pone.0013017.t003

Table 3 have trimethylation solely on K4 (Fig. 3C). Six genes have no histone trimethylation on K4 and K27 and the rest have bivalent K4/K27 trimethylation (Fig. 3C).

Discussion

Our genome-wide DNA methylation analysis shows that iPS and ES cells have similar methylation status although DNA methylation status of AM-iPS cells was closer to that of MRC-iPS cells than to that of ES cells in a small fraction. Doi et al. reported 71 differential methylated regions covering 64 genes between human iPS cells and ES cells [23]. Comparison of 535 aberrant DMSs (overlapping, 155; MRC-iPS specific, 125; AM-iPS specific, 255) with Doi's data, six genes that are *HOXA9*, *A2BP1*, *FZD10*, *SOX2*, *PTPRT* and *HYPK* overlapped. The inconsistency of most DMSs may be due to the stochastic nature of aberrant methylation through the genome. Human iPS and ES cells have general hyper-methylated status compared with differentiated cells. Our present genome-wide study indicates that pluripotent stem cells are generally hyper-methylated at promoter regions in comparison with differentiated cells. In the SS-DMRs, the number of CpG sites on non-CpG islands is grater than those on CpG islands, suggesting that promoter regions on non-CpG islands were more affected during reprogramming towards pluripotent stem cells. This result is consistent with the suggestion by Fouse et al. (2008) [24] that DNA methylation in mouse ES cells primarily occurred on non-CpG island regions of promoters.

Gene ontology analysis shows that signal transduction and transmembrane are major keywords for SS-hyper-DMRs. Most genes with SS-hyper-DMRs relate to differentiation. Recent studies demonstrate that blocking the p53 and TGFß pathways improves efficiency of generation of iPS cells [25,26,27,28,29,30]. Some genes related to these pathways are included in SS-hyper-DMR. Approximately 70% of SS-hyper-DMR have no modification of H3K4 and H3K27, suggesting that most genes with SS-hyper-DMRs are rigorously turned off by DNA methylation. By combining these findings with the result of *DNMT3A*, *DNMT3B* and *DNMT3L* induction in iPS/ES cells, we suggest that SS-hyper-DMRs apparently include genes that play a role in differentiated cells. Moreover, they must be silenced by DNMTs to establish pluripotency. We then identified 43 genes with SS-hyper-DMRs from "genes significantly suppressed in iPS/ES cells" (Table S3B and S4). In particular, *GBP3* and *SP100* could be used as epigenetic markers for pluripotency.

In addition, we successfully determined 23 genes with SS-hypo-DMRs from "genes significantly expressed in iPS/ES cells" (Table 3 and Table S3A). Those genes may start to be induced by demethylation and a significant subset of genes that act for de-

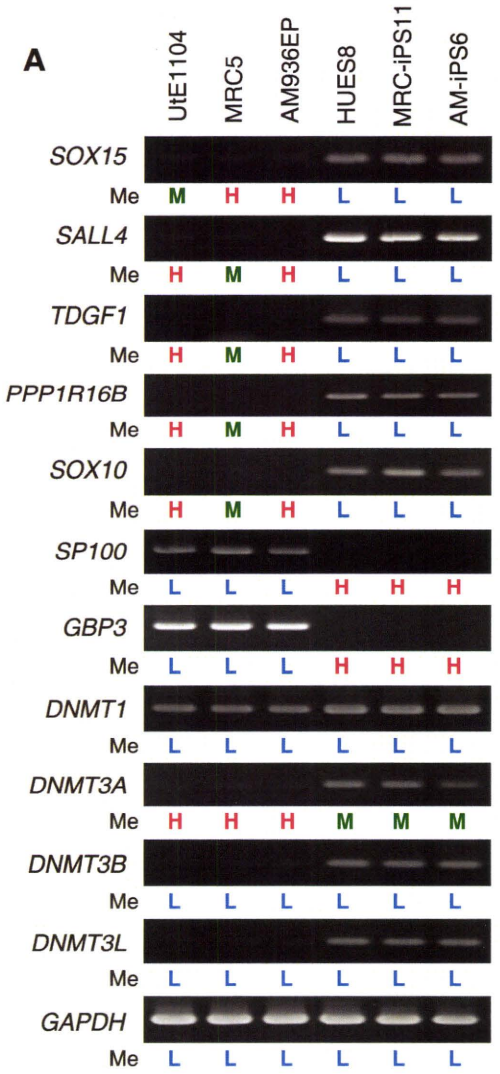

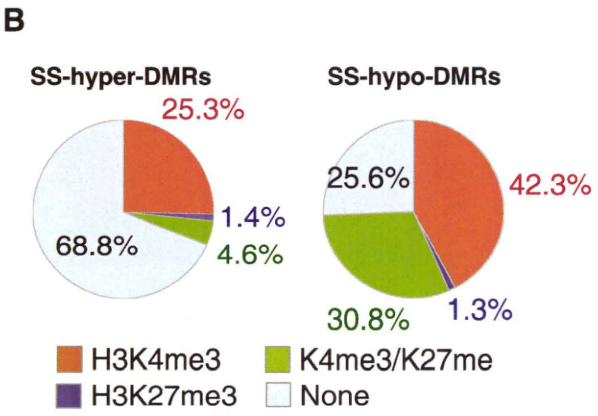

C

Histone modification of 23 genes in Table 3

H3K4me3		H3K4/K27me3	None
BCOR	C14orf115	ECL1	ANXA9
DAPK1	DNMT3A	GAL	PIPOX
GNAS	GPR160	KLNJ4	SALL4
PPP1R16B	RAB25	LRRC4	SOX10
SOX15	TDGF1		TM7SM2
POU5F1	FOXH1		VAMp8
CBX2			

Figure 3. Expression and histone modification of the SS-DMRs related genes. (**A**) Expression patterns of representative genes. RT-PCR analysis of 7 representative genes and methyltransferase genes. Methylation levels (Me) of each promoter are shown under each panel. H = High methylation (0.7<score); M = Middle methylation (0.3<score≤0.7); L = Low methylation (score≤0.3). (**B**) Comparable distribution of the SS-DMR and histone trimethylation (me3) of H3K4 and H3K27. Percentage of H3K4me3, H3K27me3, bivalent H3K4me3/K27me3 or non-modification on genes in SS-hyper-DMRs and in SS-hypo-DMRs. (**C**) Histone modification of 23 genes in Table 3.
doi:10.1371/journal.pone.0013017.g003

differentiation escape methylation in pluripotent stem cells during global reprogramming. Promoters of most marker genes expressed in human iPS/ES cells were low methylated in all cells examined (Table S5C). Analysis of histone modification of H3K4me3 and K27me3 from the database suggested that expression of *DNMT3B* might be regulated by methylation of H3K4 but expression of *DNMT3L* might not be under control of histone modification of H3K4me3 and K27me3. Most genes with SS-hypo-DMRs without expression in human iPS/ES cells have modification of H3K4me, bivalent H3K4me/K27me, or none, but do not have H3K27me3 modification. These genes may therefore be ready to be activated upon differentiation.

These findings are in generally consistent with the previous reports that have compared methylation profiles in somatic cells, iPS cells, and ES cells [23,31,32]. However, their analyses were limited only to human fibroblasts as a source for generation of iPS cells. In this study, we analyzed human extra-embryonic amnion cells and iPS cells. The DNA methylation profile at promoter sites clearly distinguished human pluripotent stem cells from differentiated cells. The SS-DMRs defined in this experiment can be used as a signature for "stemness". In addition, knowledge of the DNA methylation profile in human ES and iPS cells derived from different cell types is absolutely imperative and may allow us to screen for optimum iPS/ES cells and to validate and monitor iPS/ES cell derivatives for human therapeutic applications.

Materials and Methods

Human Cells

Human endometrium, bone marrow stroma, auricular cartilage, extra finger bone marrow, amnion, placental artery endothelium and menstrual blood cells were collected by scraping tissues from surgical specimens as a therapy, under signed informed consent, with ethical approval of the Institutional Review Board of the National Institute for Child Health and Development, Japan. Signed informed consent was obtained from

donors, and the surgical specimens were irreversibly de-identified. All experiments handling human cells and tissues were performed in line with Tenets of the Declaration of Helsinki. Endometrium (UtE1104), bone marrow stroma (H4-1) [33], auricular cartilage (Mim1508E), extra finger bone marrow (Yub636BM), amnion (AM936EP), placental artery endothelium (PAE551) and menstrual blood cell (Edom22) [34] cell lines were independently established in our laboratory. H4-1, Mim1508E, Yub636BM, AM936EP, Edom22, and MRC-5 [35] cells were maintained in the POWEREDBY10 medium (MED SHIROTORI CO., Ltd, Tokyo, Japan). PAE551 were cultured in EGM-2MV BulletKit (Lonza, Walkersville, MD, USA) containing 5% FBS. Human induced pluripotent stem (iPS) cells were generated, via procedures described by Yamanaka and colleagues [2] with slight modification. Human iPS cell lines derived from MRC-5 were designated as MRC-iPS cells [13], also iPS cell lines from AM936EP were named as AM-iPS cells [12]. Human iPS cells were maintained in iPSellon medium (Cardio Incorporated, Osaka, Japan) supplemented with 10 ng/ml recombinant human basic fibroblast growth factor (bFGF, Wako Pure Chemical Industries, Ltd., Osaka, Japan). Frozen pellets of human ES cell (HUESCs) were kindly gifted from Drs. C. Cowan and T. Tenzan (Harvard Stem Cell Institute, Harvard University, Cambridge, MA).

Illumina Infinium HumanMethylation27 BeadChip assay

Genomic DNA was extracted from cells using the QIAamp DNA Mini Kit (Qiagen). One microgram of genomic DNA from each sample was bisulfite-converted using EZ DNA Methylation-Gold kit (Zymo Research), according to the manufacturer's recommendations. Bisulfite-converted DNA was hybridized to the HumanMethylation27 BeadChip (Illumina inc.). Methylation levels of each CpG site were determined with fluorescent signals for methylated and unmethylated alleles. Methylated and unmethylated signals were used to compute a Beta value, which was a quantitative score of DNA methylation levels ranging from "0", for completely unmethylated, to "1", for completely methylated. On the HumanMethylation27 BeadChip, oligonucleotides for 27,578 CpG sites covering more than 14,000 genes are mounted, mostly selected from promoter regions. 26,956 (97.7%) out of the 27,578 CpG sites are set at promoters and 20,006 (72.5%) sites are set on CpG islands. CpG sites with $\geq$0.05 "Detection p value" (computed from the background based on negative controls) were eliminated from the data for further analysis, leaving 24,949 valid for use with the 16 samples tested.

Analysis of DNA methylation data

To analyze DNA methylation data, we used the following web tools: TIGR MeV [36] (http://www.tm4.org/mev.html) for hierarchical clustering heat map, NIA Array [37] (http://lgsun.grc.nia.nih.gov/ANOVA/) for hierarchical clustering that classify DNA methylation data by similarity and for principal component analysis (PCA) that finds major component in data variability, DAVID Bioinformatics Resources [38] (http://david.abcc.ncifcrf.gov/home.jsp), PANTHER Classification System [39] (http://www.pantherdb.org/), WebGestalt [40] (WEB-based GEne SeT AnaLysis Toolkit) (http://bioinfo.vanderbilt.edu/webgestalt/) based on based on KEGG (Kyoto Encyclopedia of Genes and Genomes) database [41] (http://www.genome.jp/kegg/) for gene ontology analysis, the GEO database (http://www.ncbi.nlm.nih.gov/geo/) for surveying gene expression in human iPS/ES cells (accession no. GSE9832 [16] and GSE12583 [17]), and the UCSC Genome Browser website [42] (http://genome.ucsc.edu/).

RT-PCR

RNA was extracted from cells using the RNeasy Plus Mini kit (Qiagen). An aliquot of total RNA was reverse transcribed using random hexamer primers. The cDNA template was amplified using specific primers for *SOX10*, *SOX15*, *PPP1R16B*, *SALL4*, *TDGF1*, *Sp100* and *GBP3*. Expression of glyceraldehyde-3-phosphate dehydrogenase (GAPDH) was used as a positive control. Primers used in this study are summarized in Table S6A.

Quantitative combined bisulfite restriction analysis (COBRA) and bisulfite sequencing

To confirm DNA methylation state, bisulfite PCR-mediated restriction mapping (known as the COBRA method) was performed. Sodium bisulfite treatment of genomic DNA was carried out as described above. PCR amplification was performed using IMMOLASE^{TM} DNA polymerase (Bioline Ltd; London, UK) and specific primers (Table S6B). After digestion with restriction enzymes, HpyCH4IV or Taq I, quantitative-COBRA coupled with the Shimadzu MCE®-202 MultiNA platform (Shimadzu, Japan) known as the Bio-COBRA method was carried out for quantitative DNA methylation level. Information of primers and restriction enzyme is summarized in Table S6B. To determine the methylation status of individual CpG in *SOX15*, *SALL4*, *Sp100* and *GBP3*, the PCR product was gel extracted and subcloned into pGEM T Easy vector (Promega, Madison, WI), and then sequenced. Methylation sites were visualized and quality control was carried out by the web-based tool, "QUMA" (http://quma.cdb.riken.jp/) [43].

Supporting Information

Table S1 Frequency of methylation states in each cell line.
Found at: doi:10.1371/journal.pone.0013017.s001 (0.04 MB PDF)

Table S2 A list of genes with SS-hyper-DMRs and SS-hypo-DMRs on KEGG Pathway.
Found at: doi:10.1371/journal.pone.0013017.s002 (0.05 MB PDF)

Table S3 (A) DNA methylation states of 23 genes (26 CpG sites) in Table 3, (B) DNA methylation states of 43 genes (50 CpG sites) in Table S4.
Found at: doi:10.1371/journal.pone.0013017.s003 (1.61 MB PDF)

Table S4 A list of 43 genes with SS-hyper-DMRs exhibiting 'low' expression in human iPS/ES cells.
Found at: doi:10.1371/journal.pone.0013017.s004 (0.07 MB PDF)

Table S5 (A) DNA methylation states of DNA methyltransferases, (B) Histone methylation states of DNA methyltransferases, (C) DNA methylation states of marker genes in human iPS/ES cells.
Found at: doi:10.1371/journal.pone.0013017.s005 (0.57 MB PDF)

Table S6 (A) primers used for RT-PCR, and (B) primers used for COBRA.
Found at: doi:10.1371/journal.pone.0013017.s006 (0.52 MB PDF)

Data set S1 A list of overlapped aberrant DMSs.
Found at: doi:10.1371/journal.pone.0013017.s007 (0.16 MB XLS)

Data set S2 A list of MRC-iPS specific aberrant DMSs.

Found at: doi:10.1371/journal.pone.0013017.s008 (0.13 MB XLS)

Data set S3 A list of AM-iPS specific aberrant DMSs.
Found at: doi:10.1371/journal.pone.0013017.s009 (0.25 MB XLS)

Data set S4 A list of SS-hyper-DMRs.
Found at: doi:10.1371/journal.pone.0013017.s010 (0.61 MB XLS)

Data set S5 A list of SS-hypo-DMRs.
Found at: doi:10.1371/journal.pone.0013017.s011 (0.10 MB XLS)

References

1. Thomson JA, Itskovitz-Eldor J, Shapiro SS, Waknitz MA, Swiergiel JJ, et al. (1998) Embryonic stem cell lines derived from human blastocysts. Science 282: 1145–1147.
2. Takahashi K, Tanabe K, Ohnuki M, Narita M, Ichisaka T, et al. (2007) Induction of pluripotent stem cells from adult human fibroblasts by defined factors. Cell 131: 861 872.
3. Huangfu D, Osafune K, Maehr R, Guo W, Eijkelenboom A, et al. (2008) Induction of pluripotent stem cells from primary human fibroblasts with only Oct4 and Sox2. Nat Biotechnol 26: 1269–1275.
4. Dimos JT, Rodolfa KT, Niakan KK, Weisenthal LM, Mitsumoto H, et al. (2008) Induced pluripotent stem cells generated from patients with ALS can be differentiated into motor neurons. Science 321: 1218–1221.
5. Woltjen K, Michael IP, Mohseni P, Desai R, Mileikovsky M, et al. (2009) piggyBac transposition reprograms fibroblasts to induced pluripotent stem cells. Nature 458: 766–770.
6. Li E (2002) Chromatin modification and epigenetic reprogramming in mammalian development. Nat Rev Genet 3: 662–673.
7. Reik W (2007) Stability and flexibility of epigenetic gene regulation in mammalian development. Nature 447: 425–432.
8. Hattori N, Nishino K, Ko YG, Ohgane J, Tanaka S, et al. (2004) Epigenetic control of mouse Oct-4 gene expression in embryonic stem cells and trophoblast stem cells. J Biol Chem 279: 17063–17069.
9. Nishino K, Hattori N, Tanaka S, Shiota K (2004) DNA methylation-mediated control of Sry gene expression in mouse gonadal development. J Biol Chem 279: 22306–22313.
10. Zingg JM, Pedraza-Alva G, Jost JP (1994) MyoD1 promoter autoregulation is mediated by two proximal E-boxes. Nucleic Acids Res 22: 2234–2241.
11. Tada M, Takahama Y, Abe K, Nakatsuji N, Tada T (2001) Nuclear reprogramming of somatic cells by in vitro hybridization with ES cells. Curr Biol 11: 1553–1558.
12. Nagata S, Toyoda M, Yamaguchi S, Hirano K, Makino H, et al. (2009) Efficient reprogramming of human and mouse primary extra-embryonic cells to pluripotent stem cells. Genes Cells 14: 1395–1404.
13. Makino H, Toyoda M, Matsumoto K, Saito H, Nishino K, et al. (2009) Mesenchymal to embryonic incomplete transition of human cells by chimeric OCT4/3 (POU5F1) with physiological co-activator EWS. Exp Cell Res 315: 2727–2740.
14. Cowan CA, Klimanskaya I, McMahon J, Atienza J, Witmyer J, et al. (2004) Derivation of embryonic stem-cell lines from human blastocysts. N Engl J Med 350: 1353–1356.
15. Brena RM, Auer H, Kornacker K, Plass C (2006) Quantification of DNA methylation in electrofluidics chips (Bio-COBRA). Nat Protoc 1: 52–58.
16. Park IH, Zhao R, West JA, Yabuuchi A, Huo H, et al. (2008) Reprogramming of human somatic cells to pluripotency with defined factors. Nature 451: 141–146.
17. Aasen T, Raya A, Barrero MJ, Garreta E, Consiglio A, et al. (2008) Efficient and rapid generation of induced pluripotent stem cells from human keratinocytes. Nat Biotechnol 26: 1276–1284.
18. Sperger JM, Chen X, Draper JS, Antosiewicz JE, Chon CH, et al. (2003) Gene expression patterns in human embryonic stem cells and human pluripotent germ cell tumors. Proc Natl Acad Sci U S A 100: 13350–13355.
19. Barski A, Cuddapah S, Cui K, Roh TY, Schones DE, et al. (2007) High-resolution profiling of histone methylations in the human genome. Cell 129: 823–837.
20. Mikkelsen TS, Ku M, Jaffe DB, Issac B, Lieberman E, et al. (2007) Genome-wide maps of chromatin state in pluripotent and lineage-committed cells. Nature 448: 553–560.
21. Bibikova M, Laurent LC, Ren B, Loring JF, Fan JB (2008) Unraveling epigenetic regulation in embryonic stem cells. Cell Stem Cell 2: 123–134.
22. Zhao XD, Han X, Chew JL, Liu J, Chiu KP, et al. (2007) Whole-genome mapping of histone H3 Lys4 and 27 trimethylations reveals distinct genomic compartments in human embryonic stem cells. Cell Stem Cell 1: 286–298.

Acknowledgments

We would like to express our sincere thanks to Drs. M. Yamada and K Miyado for discussion and critical reading of the manuscript, to Drs. C. Cowan and T. Tenzan for HUES cell lines, to Dr. D. Kami for establishing the PAE551 cell line, to K. Miyamoto for bisulfite sequencing, to Drs. K. Hata and K. Nakabayashi for COBRA.

Author Contributions

Conceived and designed the experiments: KN AU. Performed the experiments: KN MT MYI. Analyzed the data: KN YT. Contributed reagents/materials/analysis tools: KN MT MYI HM YF EC YM HO NK HA. Wrote the paper: KN AU.

23. Doi A, Park IH, Wen B, Murakami P, Aryee MJ, et al. (2009) Differential methylation of tissue- and cancer-specific CpG island shores distinguishes human induced pluripotent stem cells, embryonic stem cells and fibroblasts. Nat Genet 41: 1350–1353.
24. Fouse SD, Shen Y, Pellegrini M, Cole S, Meissner A, et al. (2008) Promoter CpG methylation contributes to ES cell gene regulation in parallel with Oct4/Nanog, PcG complex, and histone H3 K4/K27 trimethylation. Cell Stem Cell 2: 160–169.
25. Hong H, Takahashi K, Ichisaka T, Aoi T, Kanagawa O, et al. (2009) Suppression of induced pluripotent stem cell generation by the p53-p21 pathway. Nature 460: 1132–1135.
26. Kawamura T, Suzuki J, Wang YV, Menendez S, Morera LB, et al. (2009) Linking the p53 tumour suppressor pathway to somatic cell reprogramming. Nature 460: 1140–1144.
27. Utikal J, Polo JM, Stadtfeld M, Maherali N, Kulalert W, et al. (2009) Immortalization eliminates a roadblock during cellular reprogramming into iPS cells. Nature 460: 1145–1148.
28. Marion RM, Strati K, Li H, Murga M, Blanco R, et al. (2009) A p53-mediated DNA damage response limits reprogramming to ensure iPS cell genomic integrity. Nature 460: 1149–1153.
29. Li H, Collado M, Villasante A, Strati K, Ortega S, et al. (2009) The Ink4/Arf locus is a barrier for iPS cell reprogramming. Nature 460: 1136–1139.
30. Maherali N, Hochedlinger K (2009) Tgfbeta Signal Inhibition Cooperates in the Induction of iPSCs and Replaces Sox2 and cMyc. Curr Biol 18: 1718 1723.
31. Bibikova M, Chudin E, Wu B, Zhou L, Garcia EW, et al. (2006) Human embryonic stem cells have a unique epigenetic signature. Genome Res 16: 1075–1083.
32. Deng J, Shoemaker R, Xie B, Gore A, LeProust EM, et al. (2009) Targeted bisulfite sequencing reveals changes in DNA methylation associated with nuclear reprogramming. Nat Biotechnol 27: 353–360.
33. Mori T, Kiyono T, Imabayashi H, Takeda Y, Tsuchiya K, et al. (2005) Combination of hTERT and bmi-1, E6, or E7 induces prolongation of the life span of bone marrow stromal cells from an elderly donor without affecting their neurogenic potential. Mol Cell Biol 25: 5183 5195.
34. Cui CH, Uyama T, Miyado K, Terai M, Kyo S, et al. (2007) Menstrual blood-derived cells confer human dystrophin expression in the murine model of Duchenne muscular dystrophy via cell fusion and myogenic transdifferentiation. Mol Biol Cell 18: 1586–1594.
35. Jacobs JP, Jones CM, Baille JP (1970) Characteristics of a human diploid cell designated MRC-5. Nature 227: 168–170.
36. Saeed AI, Sharov V, White J, Li J, Liang W, et al. (2003) TM4: a free, open-source system for microarray data management and analysis. Biotechniques 34: 374–378.
37. Sharov AA, Dudekula DB, Ko MS (2005) A web-based tool for principal component and significance analysis of microarray data. Bioinformatics 21: 2548–2549.
38. Huang da W, Sherman BT, Lempicki RA (2009) Systematic and integrative analysis of large gene lists using DAVID bioinformatics resources. Nat Protoc 4: 44–57.
39. Mi H, Lazareva-Ulitsky B, Loo R, Kejariwal A, Vandergriff J, et al. (2005) The PANTHER database of protein families, subfamilies, functions and pathways. Nucleic Acids Res 33: D284–288.
40. Zhang B, Kirov S, Snoddy J (2005) WebGestalt: an integrated system for exploring gene sets in various biological contexts. Nucleic Acids Res 33: W741–748.
41. Kanehisa M, Araki M, Goto S, Hattori M, Hirakawa M, et al. (2008) KEGG for linking genomes to life and the environment. Nucleic Acids Res 36: D480–484.
42. Kent WJ, Sugnet CW, Furey TS, Roskin KM, Pringle TH, et al. (2002) The human genome browser at UCSC. Genome Res 12: 996–1006.
43. Kumaki Y, Oda M, Okano M (2008) QUMA: quantification tool for methylation analysis. Nucleic Acids Res 36: W170–175.

THE JOURNAL OF IMMUNOLOGY

Altered Effector $CD4^+$ T Cell Function in IL-21R $^{-/-}$ $CD4^+$ T Cell-Mediated Graft-Versus-Host Disease

Iekuni Oh, Katsutoshi Ozaki, Akiko Meguro, Keiko Hatanaka, Masanori Kadowaki, Haruko Matsu, Raine Tatara, Kazuya Sato, Yoichiro Iwakura, Susumu Nakae, Katsuko Sudo, Takanori Teshima, Warren J. Leonard and Keiya Ozawa

J Immunol 2010;185;1920-1926; Prepublished online 23 June 2010;
doi:10.4049/jimmunol.0902217
http://www.jimmunol.org/content/185/3/1920

The Journal of Immunology is published twice each month by
The American Association of Immunologists, Inc.,
9650 Rockville Pike, Bethesda, MD 20814-3994.

Print ISSN: 0022-1767 Online ISSN: 1550-6606.

Altered Effector CD4$^+$ T Cell Function in IL-21R$^{-/-}$ CD4$^+$ T Cell-Mediated Graft-Versus-Host Disease

Iekuni Oh,* Katsutoshi Ozaki,* Akiko Meguro,* Keiko Hatanaka,* Masanori Kadowaki,† Haruko Matsu,* Raine Tatara,* Kazuya Sato,* Yoichiro Iwakura,‡ Susumu Nakae,§ Katsuko Sudo,¶ Takanori Teshima,† Warren J. Leonard,‖ and Keiya Ozawa*

We previously showed that transplantation with *IL-21R* gene-deficient splenocytes resulted in less severe graft-versus-host disease (GVHD) than was observed with wild type splenocytes. In this study, we sought to find mechanism(s) explaining this observation. Recipients of donor CD4$^+$ T cells lacking IL-21R exhibited diminished GVHD symptoms, with reduced inflammatory cell infiltration into the liver and intestine, leading to prolonged survival. After transplantation, CD4$^+$ T cell numbers in the spleen were reduced, and MLR and cytokine production by CD4$^+$ T cells were impaired. These results suggest that IL-21 might promote GVHD through enhanced production of effector CD4$^+$ T cells. Moreover, we found that CD25 depletion altered neither the impaired MLR in vitro nor the ameliorated GVHD symptoms in vivo. Thus, the attenuated GVHD might be caused by an impairment of effector T cell differentiation itself, rather than by an increase in regulatory T cells and suppression of effector T cells. ***The Journal of Immunology*****, 2010, 185: 1920–1926.**

Interleukin-21 was discovered as a costimulatory cytokine for T cell proliferation and NK cell expansion in vitro (1, 2). IL-21 is produced by activated CD4 T cells (1), and its receptor is expressed on T, B, and NK cells (1, 3). It was also reported that IL-21 suppresses dendritic cell function (4) and increases hematopoietic progenitor cells (5). IL-21 is known to play critical roles in Ig production (6), whereas reports have differed regarding its contributions to Th1-, Th2-, and Th17-mediated effects and differentiation (6–15). IL-21 contributes to Th17 differentiation, but it may not be required for this process (7, 9, 14, 15). A relationship between IL-21 and autoimmune disease has been established. Overexpression of IL-21 induces inflammation, and in a systemic lupus erythematosus model mouse (the BXSB.6-Yaa$^+$/J) with high serum levels of IL-21 (16), the development of disease is abrogated when these mice are crossed to IL-21R knockout (KO) mice (17). In addition, autoimmune NOD mice do not develop diabetes in the absence of IL-21 signaling (18–20).

Graft-versus-host disease (GVHD) is a major complication following hematopoietic stem cell transplantation (21), sometimes with a fatal outcome. Previously, we showed that transplantation with *IL-21R* gene-disrupted splenocytes resulted in less severe GVHD than was seen with wild type (WT) splenocytes (22). We sought to elucidate the mechanism(s) for this observation; in this article, we demonstrate dysregulated effector function of activated CD4$^+$ T cells in IL-21R$^{-/-}$ mice.

Materials and Methods

Mice

IL-21R$^{-/-}$ and IL-17$^{-/-}$ mice were generated previously (6, 23). Both were on a C57BL/6 background. Male and female mice were used as donors. C57BL/6-DBA2-F1 male mice were purchased from Clea Japan (Tokyo, Japan). All mice used in experiments were 6–12 wk old. All mice were housed in a Jichi Medical University mouse facility, which is regulated by an intramural small animal committee, and were treated in accordance with university guidelines.

In vitro T cell stimulation and MLR

Cells were cultured in RPMI 1640 (Invitrogen, Carlsbad, CA) supplemented with 10% FCS (Sigma-Aldrich, St. Louis, MO), 2 mM L-glutamine (Invitrogen), 50 μM 2-ME (Sigma-Aldrich), 0.1 mg/ml streptomycin, and 100 U/ml penicillin G (Invitrogen). Nonspecific pan T cell stimulation was performed using anti-CD3/CD28 beads for 3 d, according to the manufacturer's instructions (Dynal Biotech, Oslo, Norway). Alloantigen-specific T cell stimulation was induced by cocultivation of CD4 T cells with 30 Gy-irradiated splenocytes from C57BL/6-DBA2-F1 mice for 4 d.

GVHD models

We used IL-21R$^{-/-}$ bone marrow (BM) to eliminate the effects of WT T cells in BM. We compared transplantations with IL-21R$^{-/-}$ CD4$^+$ T cells versus WT CD4$^+$ T cells. C57BL/6-DBA2-F1 mice were irradiated with 11 Gy and injected i.v. with 5×10^6 IL-21R$^{-/-}$ BM and 5×10^6 purified CD4$^+$ T cells from WT or IL-21R$^{-/-}$ mice. The cells were purified using CD4 microbeads and AutoMACS (Miltenyi Biotec, Tokyo, Japan); the purity was >80–90%.

Pathological analysis

Two weeks after transplantation, mice were sacrificed; liver, skin, and intestine were subjected to formalin fixation, paraffin embedding, excision, and H&E staining. Photographs were taken with an Olympus BX51 microscope at ×400 magnification.

Flow cytometric analysis

Fc-block (BD Biosciences, San Jose, CA) was used to prevent nonspecific Ab binding to Fc receptors. Abs to CD4 (RM4-5), CD8 (Ly-2), CD25

*Division of Hematology, Department of Medicine, Jichi Medical University, Tochigi; †Department of Medicine and Biosystemic Science, Kyushu University Graduate School of Medical Science, Fukuoka; ‡Center for Experimental Medicine and §Frontier Research Initiative, Institute of Medical Science, University of Tokyo; ¶Animal Research Center, Tokyo Medical University, Tokyo, Japan; and ‖Laboratory of Molecular Immunology, National Heart, Lung, and Blood Institute, National Institutes of Health, Bethesda, MD 20892

Received for publication July 14, 2009. Accepted for publication May 10, 2010.

This work was supported in part by grants from the Ministry of Health, Labor and Welfare of Japan; by grants-in-aid for Scientific Research from the Ministry of Education, Culture, Sports, Science and Technology of Japan; and by the Intramural Research Program of the National Heart, Lung and Blood Institute, National Institutes of Health, Bethesda, MD.

Address correspondence and reprint requests to Dr. Katsutoshi Ozaki, Division of Hematology, Department of Medicine, Jichi Medical University, 3311-1 Yakushiji, Shimotsuke-shi, Tochigi 329-0498, Japan. E-mail address: ozakikat@jichi.ac.jp

The online version of this article contains supplemental material.

Abbreviations used in this paper: BM, bone marrow; GVHD, graft-versus-host disease; KO, knockout; Treg, regulatory T; WT, wild type.

www.jimmunol.org/cgi/doi/10.4049/jimmunol.0902217

(7D4), H-2^b (AF6-88.5), H-2^d (SF1-1.1), IFN-γ (XMG1.2), and TNF-α (MP6-XT22) were purchased from BD Biosciences, and anti-Foxp3 (FJK-16a) was from eBioscience (San Diego, CA). Intracellular staining was performed with a Cytofx/Cytoperm kit (BD Biosciences), according to the manufacturer's instructions. Cells were stimulated with anti-mouse CD3/CD28 beads for 5 h in the presence of GolgiStop (BD Biosciences). The stimulation was omitted for Foxp3 intracellular staining. An LSR flow cytometer (BD Biosciences) was used for data collection, and data were analyzed using CellQuest software (BD Biosciences).

ELISA

ELISA kits for IL-2, IL-4, and IFN-γ were from BD Biosciences, and ELISA kits for IL-21, IL-17, TNF-α, and TGF-β1 were from R&D Systems (Minneapolis, MN). Concentrations were determined according to the manufacturer's instructions.

CD25 depletion in vitro and in vivo

In vitro purification of $CD4^+$ T cells and depletion of the $CD25^+CD4^+$ subpopulation were performed by cell sorting using a FACSAria (BD Biosciences), which yielded highly pure populations (>98%). In vivo CD25 depletion was performed by injecting anti-CD25 Ab, as described previously (24, 25). Briefly, a hybridoma producing anti-CD25 Ab (PC61; American Type Culture Collection, Manassas, VA) was cultured in serum-free medium (Protein-Free Hybridoma Medium-II from Invitrogen), and the Ab was purified from supernatant by ammonium sulfate precipitation and a PD10 column (GE Healthcare, Buckinghamshire, U.K.). The purified product was quantified using the Bradford assay (Bio-Rad, Hercules, CA) at OD595, and 1 mg was injected i.p. weekly from day 0 for 3 wk. Control rat nonspecific IgG was purchased from Invitrogen.

Quantitative RT-PCR

At day 21 after bone marrow transplantation, $CD25^-CD4^+$ T cells were purified by cell sorting from recipients of WT or IL-$21R^{-/-}$ $CD4^+$ T cells; RNA was isolated (RNeasy, Qiagen, Valencia, CA), reverse transcribed using the SuperScript First-Strand Synthesis System for RT-PCR (Invitrogen), and PCR amplified using TaqMan Gene Expression Assay's primer for mouse Foxp3 (Mm00475156) and β-actin (Mm00607939) and an ABI Prism 7700 sequence detection System (Applied Biosystems, Foster City, CA).

Statistical analysis

Kaplan–Meier plots were used to compare survival rates. The log-rank test was used to evaluate p values. Statistical analyses were performed using Stat Mate ver. 6 (ATMS, Tokyo, Japan). The Student t test was used; all error bars in this study represent SD, unless otherwise specified.

Results

Purified $CD4^+$ T cell transplantation and pathological analysis

Decreased GVHD was observed when we transplanted IL-21R–deficient splenocytes compared with WT bulk splenocytes (22). Although we sought to find molecular mechanism(s) for the ameliorated GVHD, no clue was immediately evident from the transplantation experiments (22). Thus, in this study, we used purified $CD4^+$ T cells instead of bulk splenocytes in an effort to augment the differences observed. We used a well-known model of $CD4^+$ T cell-mediated GVHD (26), in which C57BL/6 mice were donors, and C57BL/6-DBA2-F1 mice were recipients. In this model, the difference between WT and IL-$21R^{-/-}$ cells seemed to be greater than in the previous experiments using bulk splenocytes (22). All recipients of WT $CD4^+$ T cells died within 55 d, whereas those receiving IL-$21R^{-/-}$ $CD4^+$ T cells survived during this time period (Fig. 1*A*). Moreover, recipients of IL-$21R^{-/-}$ $CD4^+$ T cells recovered from body weight loss by day 14, but those receiving WT $CD4^+$ T cells did not recover and continued to lose weight (Fig. 1*B*). In recipients of IL-$21R^{-/-}$ $CD4^+$ T cells, pathological analysis showed markedly reduced infiltration into the regions surrounding bile ducts and portal veins and into the interstitial region of small intestine compared with the infiltration observed in recipients of WT $CD4^+$ T cells (Fig. 2, *upper* and *middle panels*). Apoptotic bodies near the surface area of crypts in the small intestine were barely visible in recipients

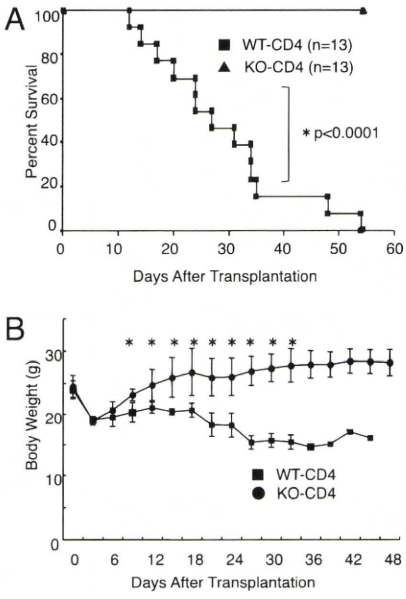

FIGURE 1. A role for IL-21 in $CD4^+$ T cell-mediated GVHD. *A*, Survival of recipients of WT and IL-$21R^{-/-}$ $CD4^+$ T cells. C57BL/6-DBA2-F1 mice were irradiated with 11 Gy and received 5×10^6 IL-$21R^{-/-}$ BM with 5×10^6 WT or IL-$21R^{-/-}$ $CD4^+$ T cells. Shown are combined data from two independent experiments. Thirteen recipients each for WT and IL-$21R^{-/-}$ $CD4^+$ T cells were analyzed. The log-rank test was used to calculate p values. *B*, Body weight after BM transplantation. Statistical significance was assessed with the Student t test.

of IL-$21R^{-/-}$ $CD4^+$ T cells, in contrast to recipients of WT $CD4^+$ T cells, in which apoptotic bodies were evident (Fig. 2, arrowheads in *middle panel*). No significant difference was observed in skin

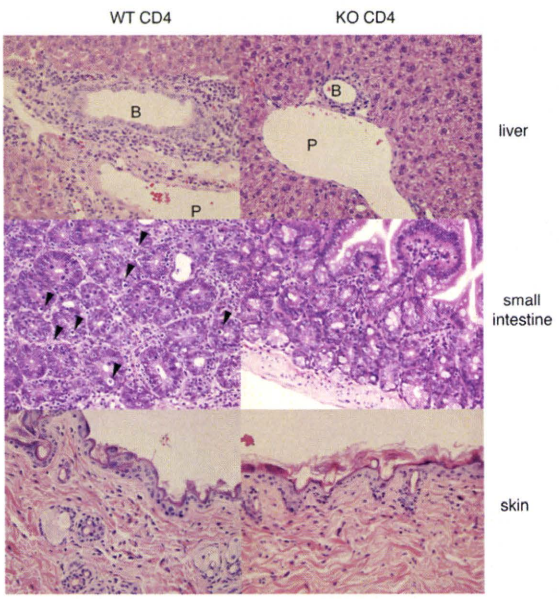

FIGURE 2. Pathological analysis of recipients. Liver, small intestine, and skin were stained with H&E (original magnification ×400). In recipients of WT $CD4^+$ T cells, cell infiltration is evident around the portal vein (P) and the bile duct (B) and into the interstitial region in small intestine. Arrowheads indicate apoptotic bodies near the surface of crypts. These changes were barely visible in recipients of IL-$21R^{-/-}$ $CD4^+$ T cells. Skin did not show any significant difference between recipients of WT and IL-$21R^{-/-}$ $CD4^+$ T cells. Shown is a representative result of six mice analyzed in each group. Only one recipient of IL-$21R^{-/-}$ $CD4^+$ T cells showed apoptotic bodies in the lumens of intestine and infiltration around the bile duct and portal vein, as was observed in the recipients of WT $CD4^+$ T cells.

pathology among recipients of WT CD4$^+$ and IL-21R$^{-/-}$ CD4$^+$ T cells. These results suggested that IL-21 might be essential for CD4-mediated GVHD, at least in this setting.

Normal cytokine production by splenocytes after transplantation is dependent on IL-21

The above observations suggested that IL-21–mediated donor CD4$^+$ T cell activation was involved in the exacerbation of GVHD. Because we could not find any significant difference in serum cytokine concentrations after transplantation (Supplemental Fig. 1), we assessed T cell differentiation by cytokine production in the presence of cellular stimulation. Interestingly, at days 14 and 21 after transplantation, bulk splenocytes from recipients of IL-21R$^{-/-}$ CD4$^+$ T cells exhibited defective cytokine production, with decreased levels of IFN-γ, TNF-α, and IL-4; in contrast, levels of IL-2, IL-17, and IL-21 were not significantly diminished (Fig. 3, *left panels*). Before transplantation, IL-21R$^{-/-}$ CD4$^+$ T cells did not show any significant defect in IFN-γ, IL-4, or TNF-α production (Fig. 3, *right panels*), suggesting that the defect was acquired after transplantation. This defect in effector T cell function might represent a mechanism for the difference in the development of GVHD by mice receiving WT versus IL-21R$^{-/-}$ CD4$^+$ T cells.

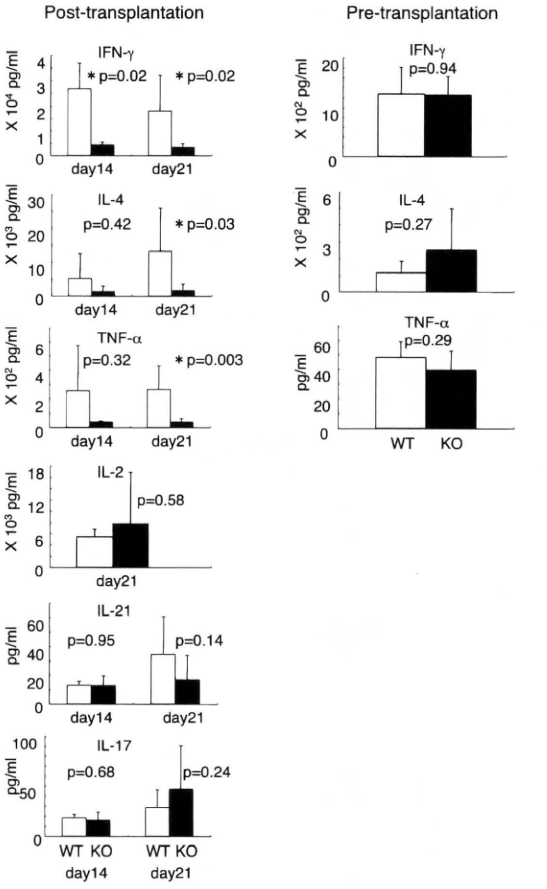

FIGURE 3. Cytokine production by bulk splenocytes before and after CD4$^+$ T cell transplantation. At days 14 and 21 after transplantation, splenocytes (5×10^5) were taken and stimulated with anti-CD3/CD28 Abs for 18 h. Concentrations of cytokines in the supernatants were determined by ELISA. Twelve or 13 recipients of WT CD4$^+$ T cells and 10 recipients of IL-21R$^{-/-}$ CD4$^+$ T cells were analyzed. Prior to transplantation, five WT and eight IL-21R$^{-/-}$ mice were analyzed. At days 14–21 after transplantation, the proportion of donor cells in the spleen was >95%. The Student *t* test was used to calculate *p* values. *Statistical significance ($p < 0.05$).

CD4$^+$ T cells were responsible for the low production of cytokines

To elucidate the basis for diminished cytokine production, we examined the number of donor CD4$^+$ T cells in the spleen at days 14–21 after transplantation. The number of donor H-2K^{d-}CD4$^+$ T cells was significantly lower in recipients of IL-21R$^{-/-}$ CD4$^+$ T cells than in recipients of WT CD4$^+$ T cells (Fig. 4*A*; $p = 0.03$, Welch *t* test; $n = 15$ versus 12), although the ranges overlapped. Because it is thought that donor T cells proliferate in secondary lymphoid organs, such as the spleen, and then infiltrate into target organs (27), the reduced number of CD4$^+$ T cells in the spleen is consistent with the reduced infiltration into the liver and small intestine, as shown above (Fig. 2). To identify the cells responsible for defective cytokine production, we performed intracellular staining and ELISA with purified CD4$^+$ T cells. After anti-CD3/CD28 stimulation, the proportion of IFN-γ$^+$ and TNF-α$^+$ cells in splenic CD4$^+$ T cells was lower in recipients of IL-21R$^{-/-}$ CD4$^+$ T cells than in those receiving WT CD4$^+$ T cells (Fig. 4*B*). Moreover, posttransplantation, the levels

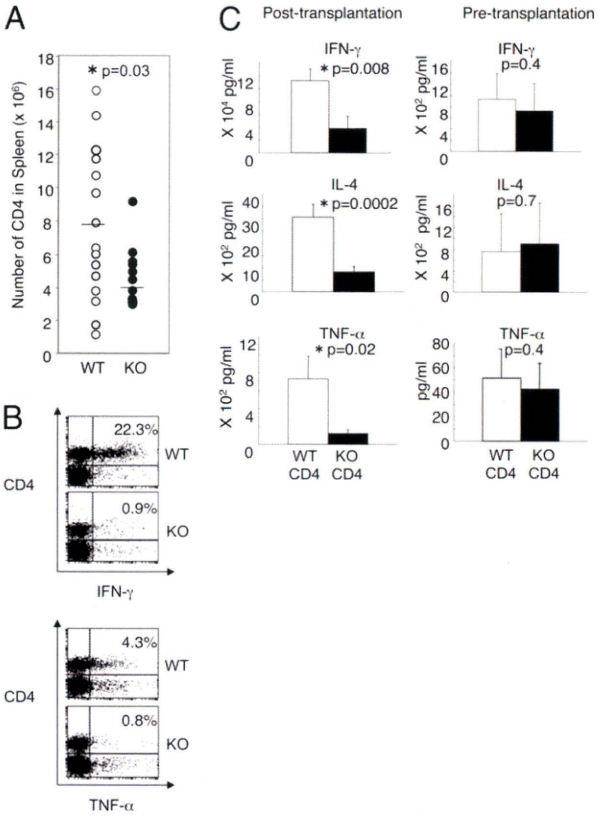

FIGURE 4. Cytokine production by splenic CD4$^+$ T cells before and after transplantation. *A*, Absolute number of donor H-2K^{d-}CD4$^+$ T cells in the spleen. The number of donor CD4$^+$ T cells was determined by multiplying the number of splenocytes by the percentage of H-2K^{d-}CD4$^+$ T cells. Each dot depicts the number of donor CD4$^+$ T cells in a mouse. Horizontal lines indicate the average. Fifteen recipients of WT CD4$^+$ T cells and 12 recipients of IL-21R$^{-/-}$ CD4$^+$ T cells were assessed. *B*, Intracellular staining of splenocytes after anti-CD3/CD28 stimulation. Splenocytes (1×10^6) were stimulated with anti-CD3/CD28 Abs for 5–6 h and stained with anti–IFN-γ or anti–TNF-α Ab in combination with anti-CD4 Ab. A total of three recipients in each group were analyzed, and a representative result is shown. *C*, Cytokine production by CD4$^+$ T cells in vitro. At days 14 or 21 after transplantation, splenic CD4$^+$ T cells (5×10^5) were purified and stimulated with anti-CD3/CD28 Abs for 18 h. Concentrations of cytokines in the supernatants were determined by ELISA. Twelve mice were analyzed in each group after transplantation. Five or six WT and eight or nine IL-21R$^{-/-}$ mice were analyzed before transplantation. *Statistical significance ($p < 0.05$).

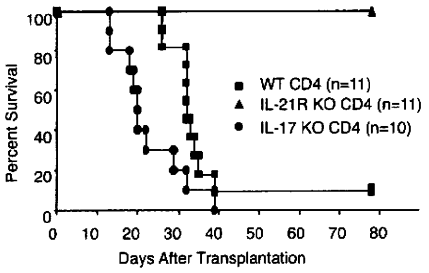

FIGURE 5. IL-17$^{-/-}$ CD4$^+$ T cells induced lethal GVHD. Survival of recipients of WT, IL-21R$^{-/-}$ (IL-21R KO), or IL-17$^{-/-}$ (IL-17 KO) CD4$^+$ T cells. Lethally irradiated (11 Gy) C57BL/6-DBA2-F1 mice were transplanted with 5 × 10^6 IL-21R KO BM and 5 × 10^6 WT, IL-21R KO, or IL-17 KO CD4$^+$ T cells. The data represent the combined results of two independent experiments.

of IFN-γ, TNF-α, and IL-4 production were significantly diminished with splenic-purified CD4$^+$ T cells from recipients of IL-21R$^{-/-}$ CD4$^+$ T cells compared with those receiving WT CD4$^+$ T cells (Fig. 4*C*, *left panels*). Before transplantation, IL-21R$^{-/-}$ CD4$^+$ T cells did not show any defect in IFN-γ, TNF-α, and IL-4 production (Fig. 4*C*, *right panels*).

IL-17 production and GVHD induced by IL-17$^{-/-}$ CD4$^+$ T cells

Although IL-21 is not essential for Th17 differentiation, IL-21 can promote it. To evaluate the effect of IL-21$^{-/-}$ CD4$^+$ T cell transplantation on IL-17 production, we measured IL-17 after transplantation. As shown in Fig 3, *bottom left panel*, bulk splenocytes from recipients of IL-21R$^{-/-}$ CD4$^+$ T cells produced comparable amounts of IL-17 at days 14 and 21 after transplantation compared with mice receiving WT CD4$^+$ T cells. Moreover, we found that IL-17$^{-/-}$ CD4$^+$ T cells induced lethal GVHD analogous to WT CD4$^+$ T cells (if anything, death occurred earlier), suggesting that IL-17 is dispensable for this process, in contrast to the essential role of IL-21, as reflected by the survival of mice receiving IL-21R$^{-/-}$ CD4$^+$ T cells (Fig. 5).

Regulatory T cell number in spleen

We next determined the serum concentration of the major immunosuppressive cytokine, TGF-β1, at days 6–21 after transplantation. We found an increase in TGF-β1 only after transplantation (Fig. 6*A*; $p = 0.0003$ at day 14; $p = 0.01$ at day 21, Student t test). In splenocytes from recipients of IL-21R$^{-/-}$ CD4$^+$ T cells, the production of TGF-β1 and IL-10 by in vitro T cell stimulation was not upregulated; in fact, it tended to be diminished (Supplemental Fig. 2), suggesting that the increase in serum TGF-β1 might be due to cells other than T cells. Because naive T cells can differentiate into regulatory T (Treg) cells in the presence of TGF-β1 (28), and it was reported that IL-21$^{-/-}$ T cells were predisposed to differentiate into Treg cells (8), we also investigated whether more Treg cells were induced in recipients of IL-21R$^{-/-}$ CD4$^+$ T cells. The proportion

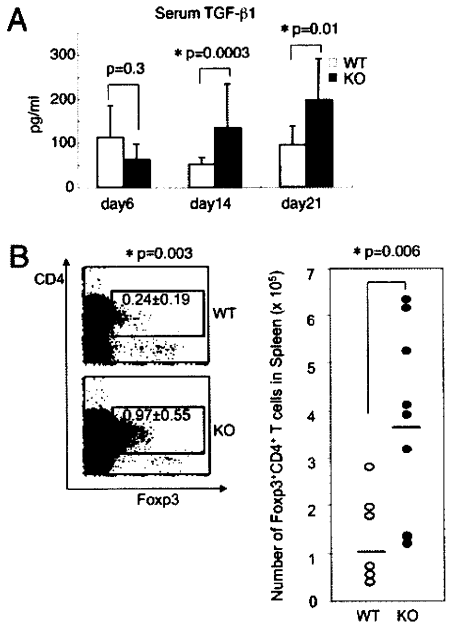

FIGURE 6. Increase in splenic Treg cells. *A*, Upregulation of serum TGF-β1. Serum TGF-β1 concentrations at the indicated day after transplantation were determined by ELISA. Three samples from recipients of WT CD4$^+$ T cells and 4 samples from recipients of IL-21R$^{-/-}$ CD4$^+$ T cells at day 6, 23 samples from recipients of WT CD4$^+$ T cells and 25 samples from recipients of IL-21R$^{-/-}$ CD4$^+$ T cells at day 14, and 8 samples from recipients of WT CD4$^+$ T cells and 7 samples from recipients of IL-21R$^{-/-}$ CD4$^+$ T cells at day 21 were analyzed. *Statistical significance ($p < 0.05$). *B*, The percentage and absolute number of splenic Foxp3$^+$CD4$^+$ regulatory T cells at day 14 after transplantation. The left panel shows a representative flow cytometric result from eight or nine similar samples. The right panel indicates the number of all samples; the averages are indicated by the horizontal lines.

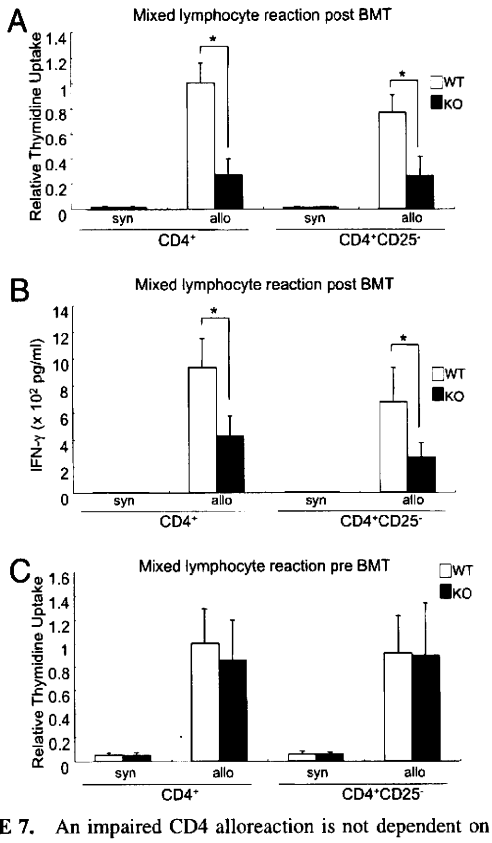

FIGURE 7. An impaired CD4 alloreaction is not dependent on CD25$^+$ CD4$^+$ T cells. CD4 alloreaction in vitro was impaired after transplantation, and this impairment was not restored by CD25$^+$ T cell depletion. *A*, At day 14 after transplantation, 1 × 10^5 sorter-purified splenic CD4$^+$ or CD25$^-$ CD4$^+$ T cells (>98% purity) were cultured with 4 × 10^5 irradiated allogeneic C57BL/6-DBA2-F1 splenocytes for 4 d. The cells were pulsed with 1 μCi of [^{3}H]thymidine for the last 24 h. Relative thymidine uptake to the value of WT CD4$^+$ T cells is depicted. *B*, Culture was the same as in *A*, but IFN-γ concentrations in the supernatants were determined by ELISA. *C*, Sorter-purified splenic CD4$^+$ or CD25$^-$CD4$^+$ cells from nontransplanted mice were cultured with irradiated allogeneic C57BL/6-DBA2-F1 splenocytes. Relative thymidine uptake to the number of WT CD4$^+$ T cells is depicted. *$p < 0.05$.

of splenic Foxp3$^+$CD4$^+$ Treg phenotype cells in recipients of IL-21R$^{-/-}$ CD4$^+$ T cells was higher than in recipients of WT CD4$^+$ T cells, but the total percentage was still only ~1% (Fig. 6*B*, *left panel*). The absolute number was ~4-fold higher, but the actual number was only ~4×10^5 of the total number of splenocytes (~4×10^7) (Fig. 6*B*, *right panel*). In contrast to posttransplantation, pretransplantation splenocytes from IL-21R$^{-/-}$ mice did not show an increase in Foxp3$^+$CD4$^+$ T cells compared with cells from WT mice (Supplemental Fig. 3), suggesting that the increased Treg cell after transplantation was an induced Treg cell during GVHD reaction. For that reason, we did not deplete CD25$^+$ cells prior to transplantation.

CD25 depletion did not restore the suppressed alloreaction in vitro and did not exacerbate the ameliorated GVHD

To investigate the importance of Treg cells in diminishing GVHD, we performed an MLR, which corresponds to alloreaction in vitro, with or without CD25$^+$CD4$^+$ T cells. Because Foxp3 is an intracellular protein, and Foxp3 staining cannot be used to purify or deplete Treg cells, anti-CD25 Ab is widely used for this purpose (9, 29–32). The impaired MLR of IL-21R$^{-/-}$ CD4$^+$ T cells after transplantation was not restored by CD25 depletion (Fig. 7*A*), nor was the impaired IFN-γ production by IL-21R$^{-/-}$CD4$^+$ T cells in an MLR (Fig. 7*B*). Moreover, analogous to cytokine production by anti-CD3/CD28 stimulation (Fig. 3), IL-21R$^{-/-}$ CD4$^+$ T cells before transplantation were not defective for alloreaction (Fig. 7*C*).

Consistent with the in vitro experiments above, CD25$^+$ depletion in vivo did not alter the severity of GVHD in recipients of IL-21R$^{-/-}$ CD4$^+$ T cells, without altering the body weight loss and survival (Fig. 8*A*, 8*B*). In contrast, the severity of GVHD in recipients of WT CD4$^+$ T cells seemed to be slightly diminished by CD25$^+$ depletion (Fig. 8*A*, 8*B*). In this condition, as previously reported (30), the depletion efficacy of CD25$^+$CD4$^+$ T cells was >95% and that of Foxp3$^+$CD4$^+$ T cells was ≥50% (Fig. 8*C*, *upper* and *lower panels*). Interestingly, Foxp3 expression was higher in CD25$^-$CD4$^+$ T cells from recipients of IL-21R$^{-/-}$ CD4$^+$ T cells than from recipients of WT CD4$^+$ T cells (Fig. 8*D*). Together with the results in vitro (Fig. 7), this suggests a relationship between the unresponsiveness of CD25$^-$CD4$^+$ T cells and greater expression of Foxp3.

Discussion

In this article, we reported evidence indicating that IL-21 is critical for the pathogenesis of CD4$^+$ T cell-mediated GVHD, at least in part because of its effects on CD4 differentiation. In this study, we focused on CD4$^+$ T cell-mediated GVHD; a role for IL-21 in CD8$^+$ T cell-mediated GVHD remains to be investigated.

We found a profound defect in T cell effector function only after transplantation, although serum cytokine concentrations showed no obvious difference. According to these results, T cell differentiation into Th1 and Th2 cells seemed to be altered in the absence of IL-21 during GVHD. Cytokines are believed to have positive and negative roles in GVHD. For example, although T cells from IFN-γ–deficient mice resulted in more severe GVHD (33–35), T cells from Stat4 (Th1)-deficient mice resulted in less severe GVHD than did T cells from WT mice with less severe colitis (36). In contrast to IFN-γ$^{-/-}$ T cells, T cells from IL-4–deficient mice induced less severe GVHD (34); analogously, T cells from Stat6 (Th2)-deficient mice induced less severe GVHD than did those from WT mice (36). T cells from TNF-α–deficient mice developed less severe GVHD, with less severe colitis (37). Our data suggest a strong correlation between the defect in effector function in recipients of IL-21R$^{-/-}$ CD4$^+$ T cells and the attenuated phenotype of GVHD, indicating a role for IL-21 in this process.

IL-21, as well as IL-6, induces Th17 differentiation in the presence of TGF-β, suggesting a possible involvement of IL-17 in

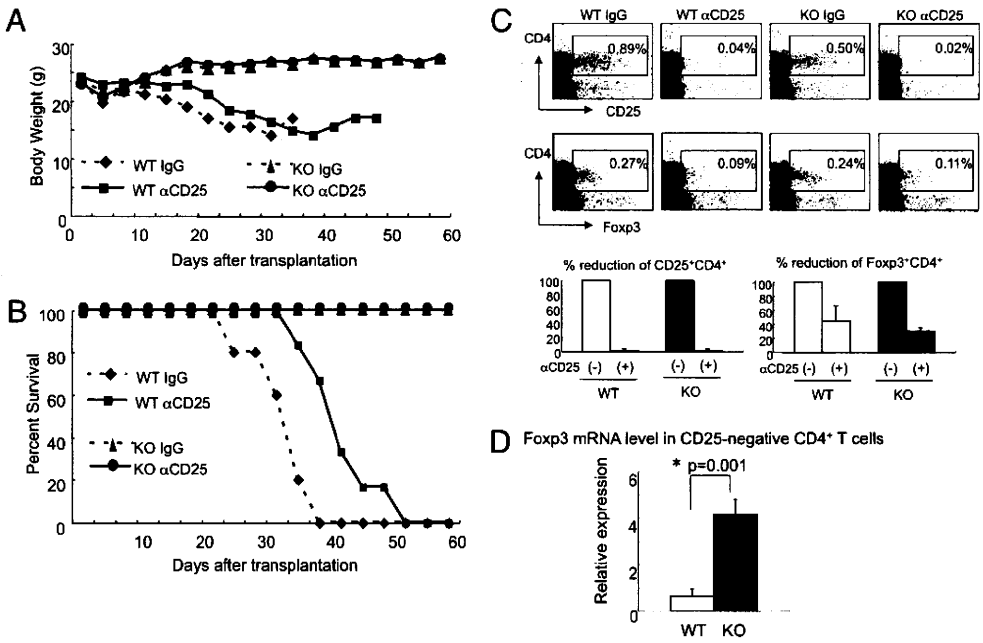

FIGURE 8. The ameliorated GVHD induced by IL-21R$^{-/-}$ CD4$^+$ T cells is not dependent on CD25$^+$CD4$^+$ T cells. The ameliorated GVHD induced by IL-21R$^{-/-}$ CD4$^+$ T cells was not exacerbated by depletion of CD25$^+$CD4$^+$ T cells. Body weight (*A*) and survival (*B*) of recipients are shown. Comparisons of recipients of WT CD4$^+$ T cells and IL-21R$^{-/-}$ CD4$^+$ T cells and additional comparisons with and without anti-CD25 Ab treatment were performed. Nonspecific rat IgG was used as the control Ab. *C*, Splenic CD25$^+$CD4$^+$ T cells and splenic Foxp3$^+$CD4$^+$ T cells at day 14 after transplantation with or without anti-CD25 Ab treatment were analyzed by flow cytometry (*upper two rows*). The lower panels indicate the mean reduction in the percentage of CD25$^+$CD4$^+$ and Foxp3$^+$CD4$^+$ cells from three similar results. *D*, Foxp3 mRNA level in CD25$^-$CD4$^+$ T cells at day 21 after transplantation. Cell sorter-purified CD25$^-$CD4$^+$ T cells were subjected to mRNA purification, reverse-transcriptase treatment, and TaqMan quantitative PCR. Relative value to β-actin is denoted.